Full-Waveform Inversion and Reverse-Time Migration in Earthquake and Exploration Seismology

Frederik J Simons

Zhaolun Liu | Qiancheng Liu | Zhendong Zhang

Alex L. Burky | Congyue Cui | Etienne Bachmann

Jessica C.E. Irving | Jürgen Hoffmann | Jeroen Tromp

Princeton University | Bristol University | DNO

Introduction – I

Introduction – I

The **geological evolution** of our *chemically differentiated* and *physically deformed* planet is recorded in the interior distribution of **compositional** and **thermal** heterogeneities.

Introduction – I

The **geological evolution** of our *chemically differentiated* and *physically deformed* planet is recorded in the interior distribution of **compositional** and **thermal** heterogeneities.

- These affect the propagation speed of **seismic waves**

Introduction – I

The **geological evolution** of our *chemically differentiated* and *physically deformed* planet is recorded in the interior distribution of **compositional** and **thermal** heterogeneities.

- These affect the propagation speed of **seismic waves**
- They cause variations in the acceleration due to **gravity**

Introduction – I

The **geological evolution** of our *chemically differentiated* and *physically deformed* planet is recorded in the interior distribution of **compositional** and **thermal** heterogeneities.

- These affect the propagation speed of **seismic waves**
- They cause variations in the acceleration due to **gravity**
- They are expressed as surface **topography** and oceanic **bathymetry**

Introduction – II

To understand Earth, and indeed any planet,

we must study all three (physical) observables:

Introduction – II

To understand Earth, and indeed any planet,

we must study all three (physical) observables:

- **(an)elastic wave speeds**

  (including attenuation & anisotropy)

Introduction – II

To understand Earth, and indeed any planet,

we must study all three (physical) observables:

- **(an)elastic wave speeds**

  (including attenuation & anisotropy)

- **mass density, gravity field**

  (static, dynamic & time-dependent)

Introduction – II

To understand Earth, and indeed any planet,

we must study all three (physical) observables:

- **(an)elastic wave speeds**

  (including attenuation & anisotropy)

- **mass density, gravity field**

  (static, dynamic & time-dependent)

- **height of mountains, depth of oceans**

  (tectonic motion, interactions with winds & currents)

Introduction – II

To understand Earth, and indeed any planet,

we must study all three (physical) observables:

- **(an)elastic wave speeds**

  (including attenuation & anisotropy)

- **mass density, gravity field**

  (static, dynamic & time-dependent)

- **height of mountains, depth of oceans**

  (tectonic motion, interactions with winds & currents)

and how they **correlate**, at any and all **scales**.

Chemistry & Thermodynamics $\rightarrow$ Physical Properties

Temperature / Pressure

(*how hot is it deep down there?*)

Chemistry & Thermodynamics $\rightarrow$ Physical Properties

Temperature / Pressure

(*how hot is it deep down there?*)

Composition / Phase changes

(*what is it all made of and how?*)

Chemistry & Thermodynamics $\longrightarrow$ Physical Properties

Temperature / Pressure

(*how hot is it deep down there?*)

Composition / Phase changes

(*what is it all made of and how?*)

$\downarrow$

Mass density ($\mathrm{kg\,m^{-3}}$)

Seismic wave speeds ($\mathrm{m\,s^{-1}}$)

One hundred thousand earthquakes

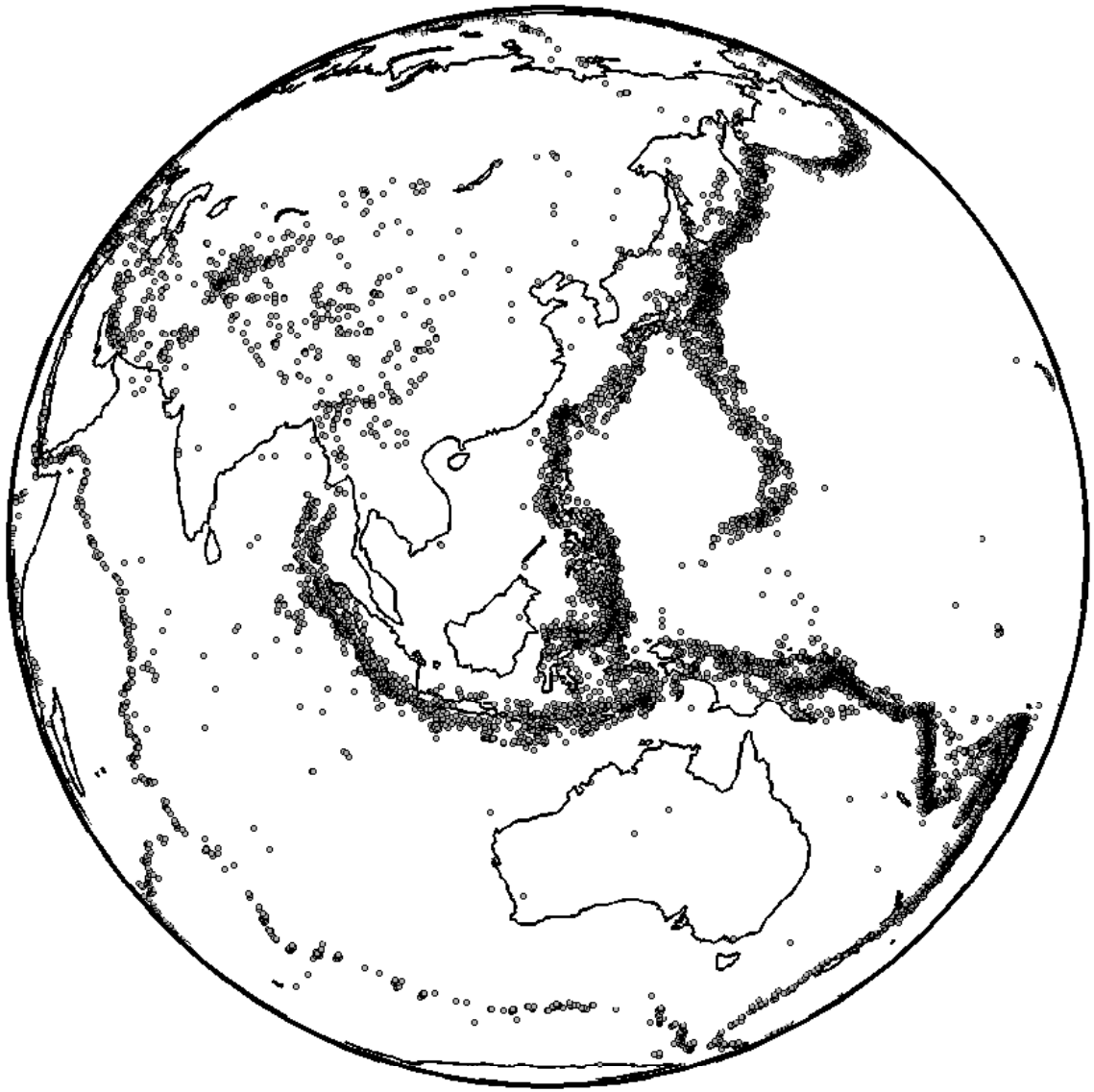

One hundred thousand earthquakes

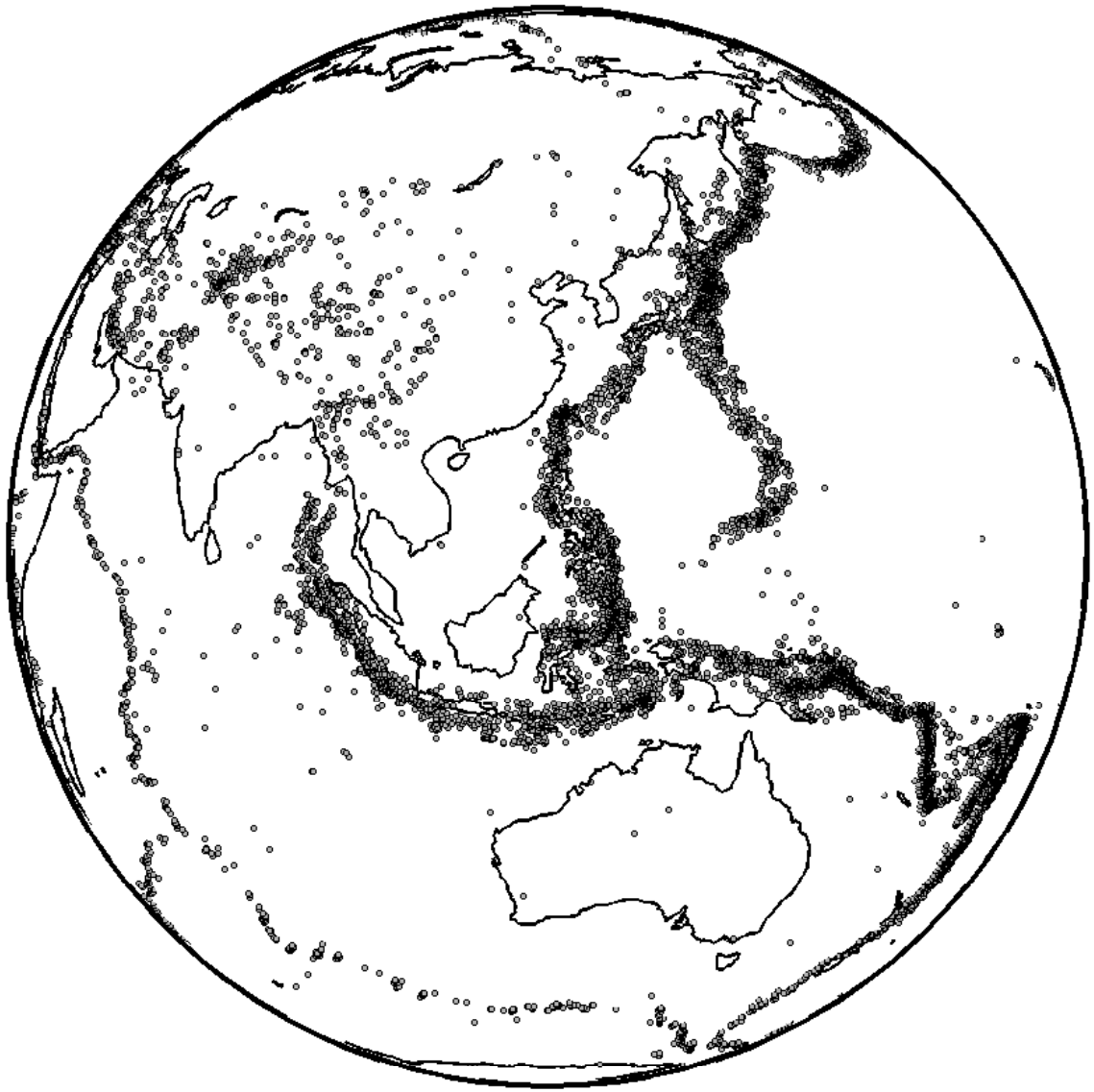

$N \approx 2/\text{day}$

Ekström et al. (2012)

A rich and rewarding wavefield

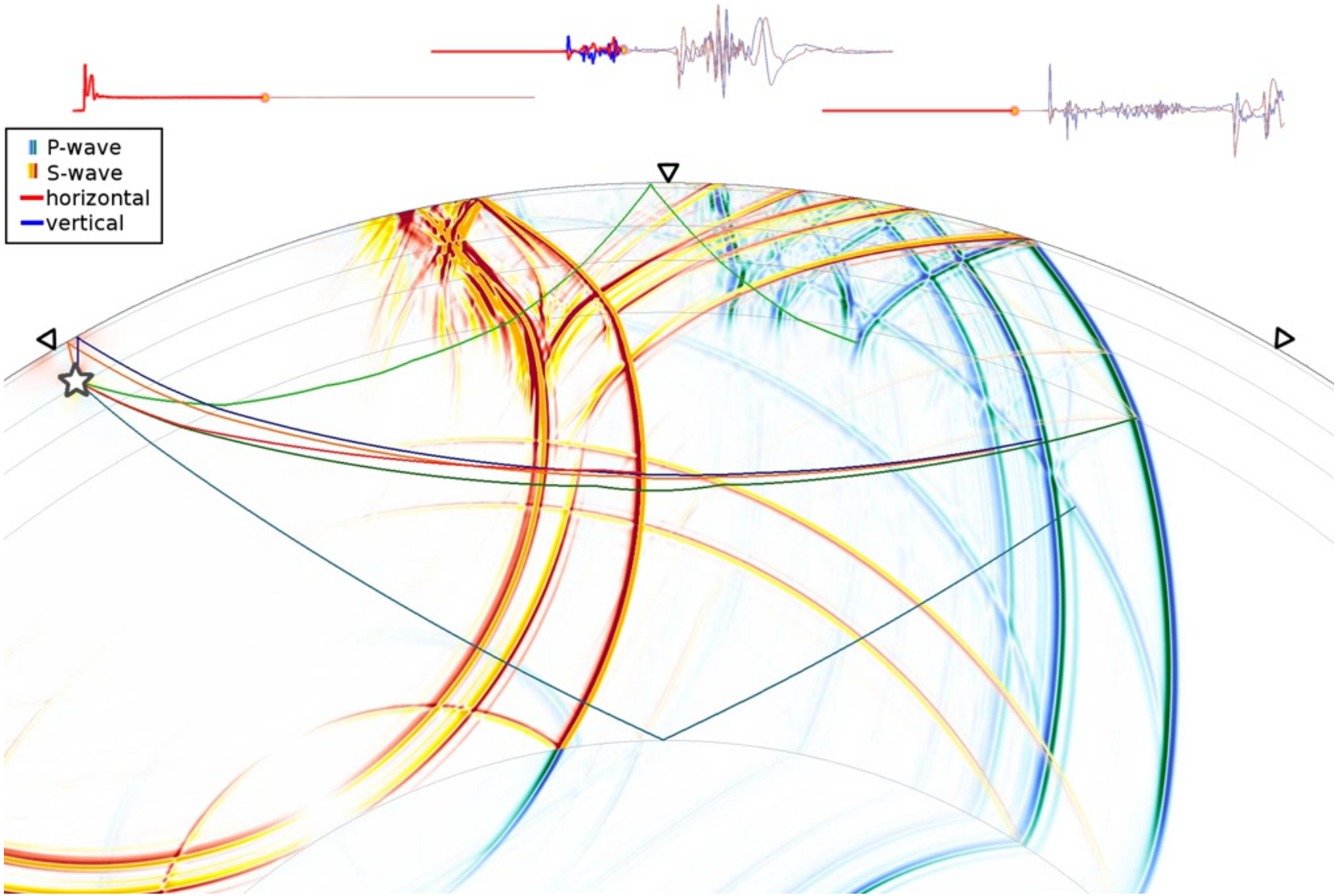

Nissen-Meyer et al. (2014)

Thousands of seismometers

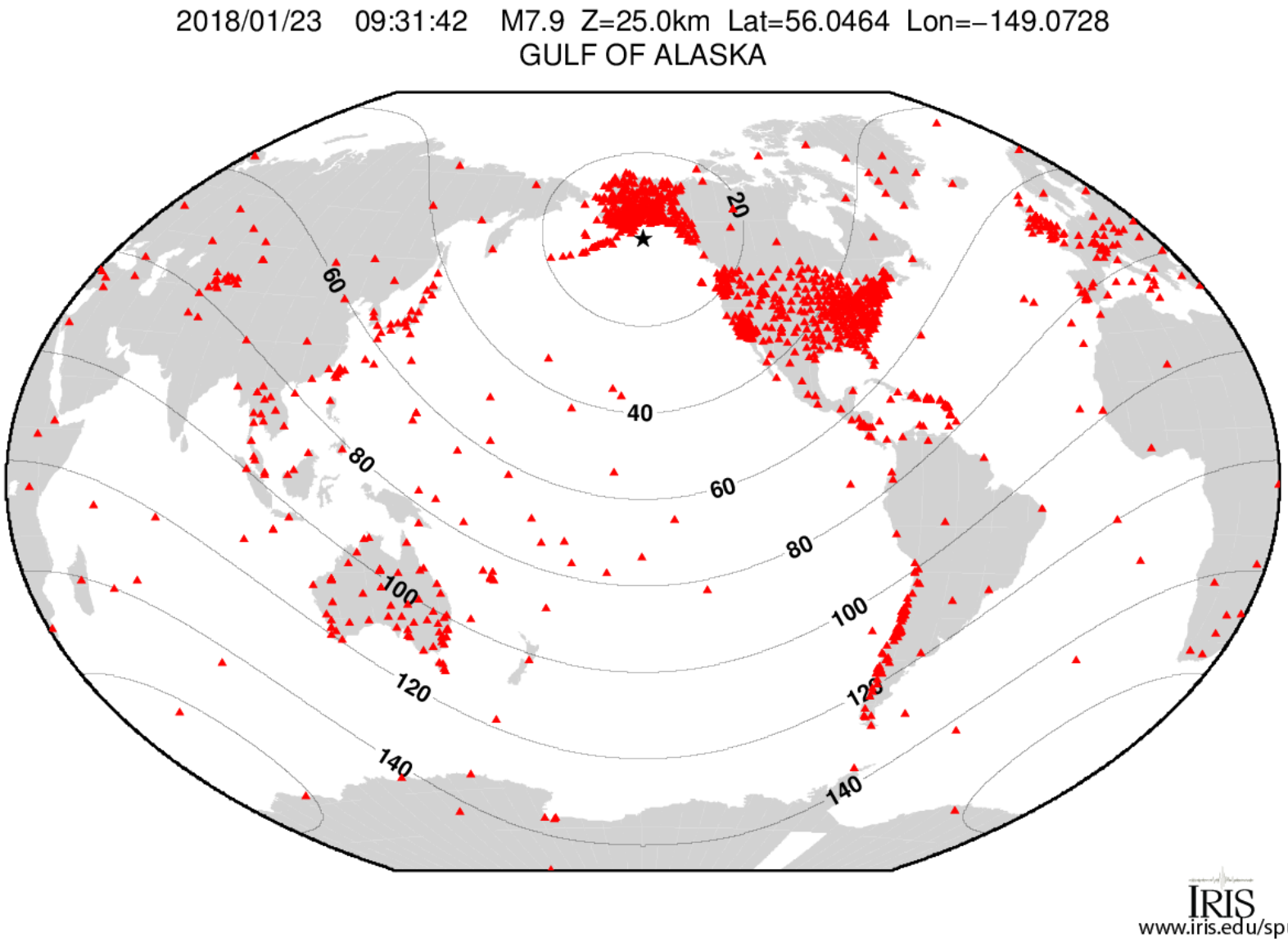

Hundreds of identifiable phases

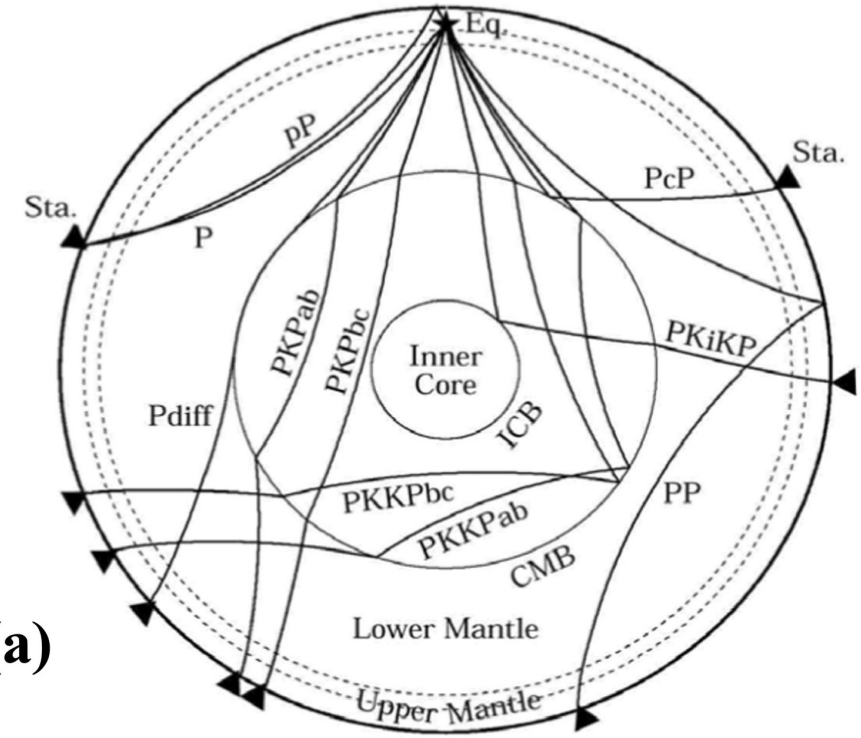

(a)

Hundreds of identifiable phases

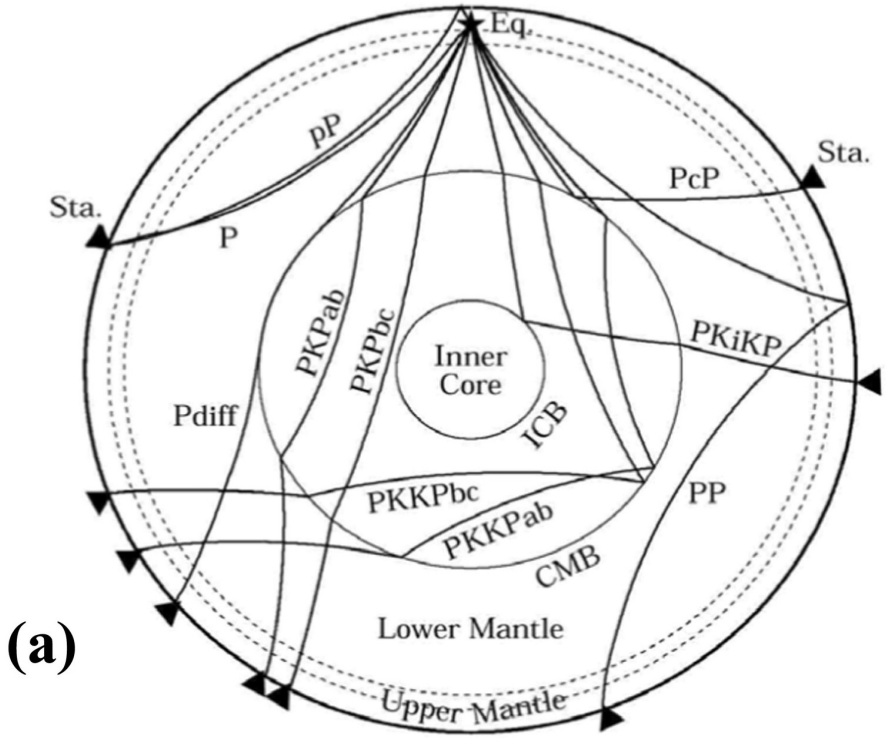

(a)

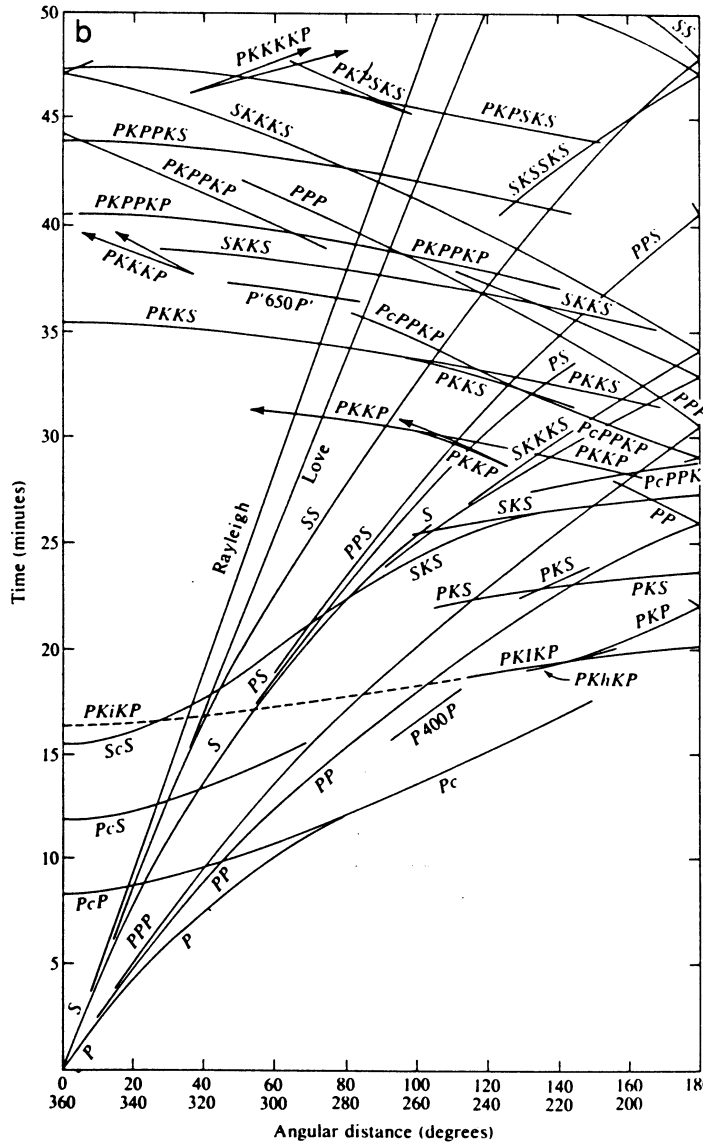

Bullen and Bolt (1985); *Zhao* (2019)

One-dimensional reference Earth models

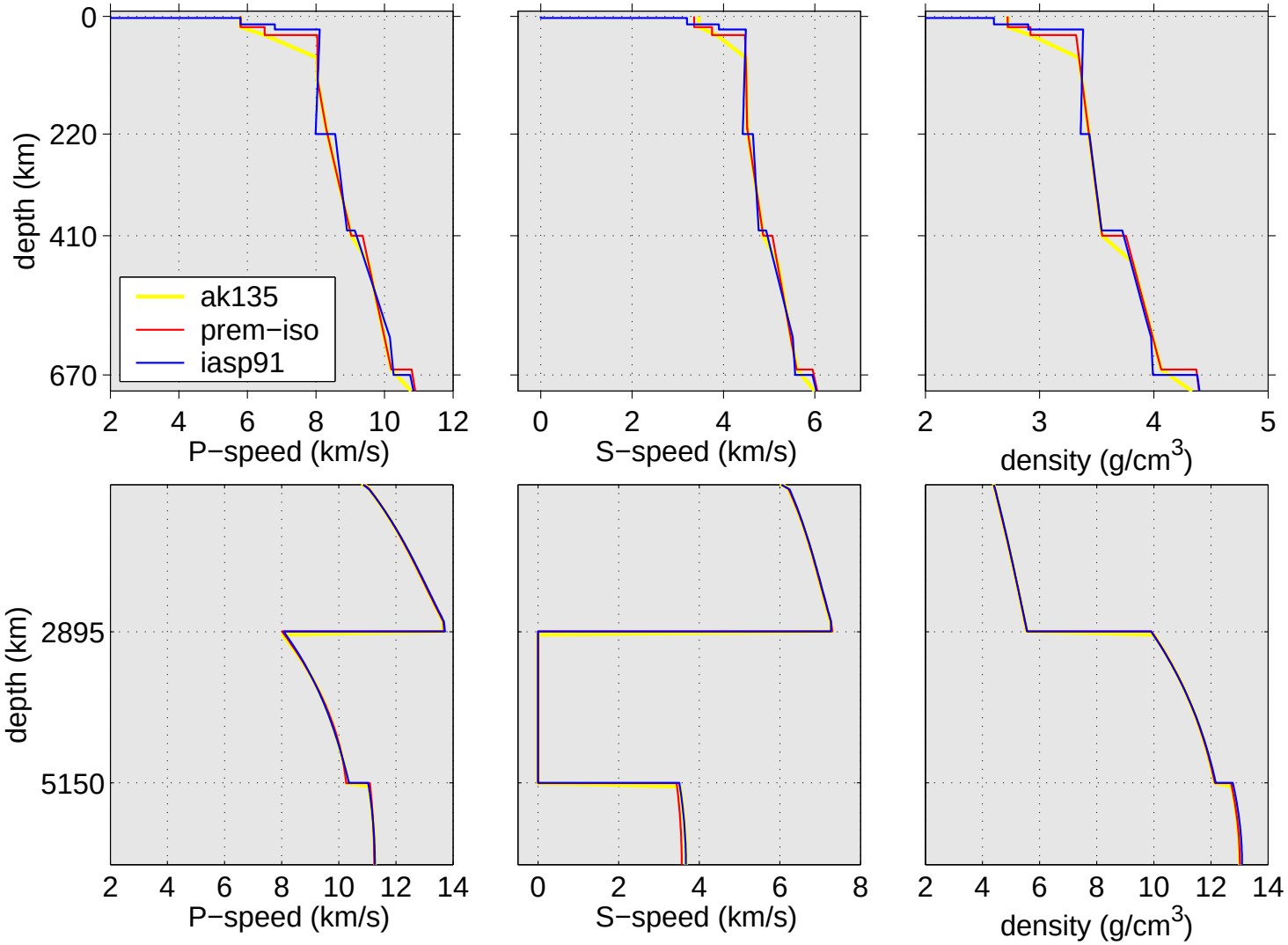

Dziewoński and Anderson (1981); *Kennett and Engdahl* (1991)

Millions of travel times (signal?)

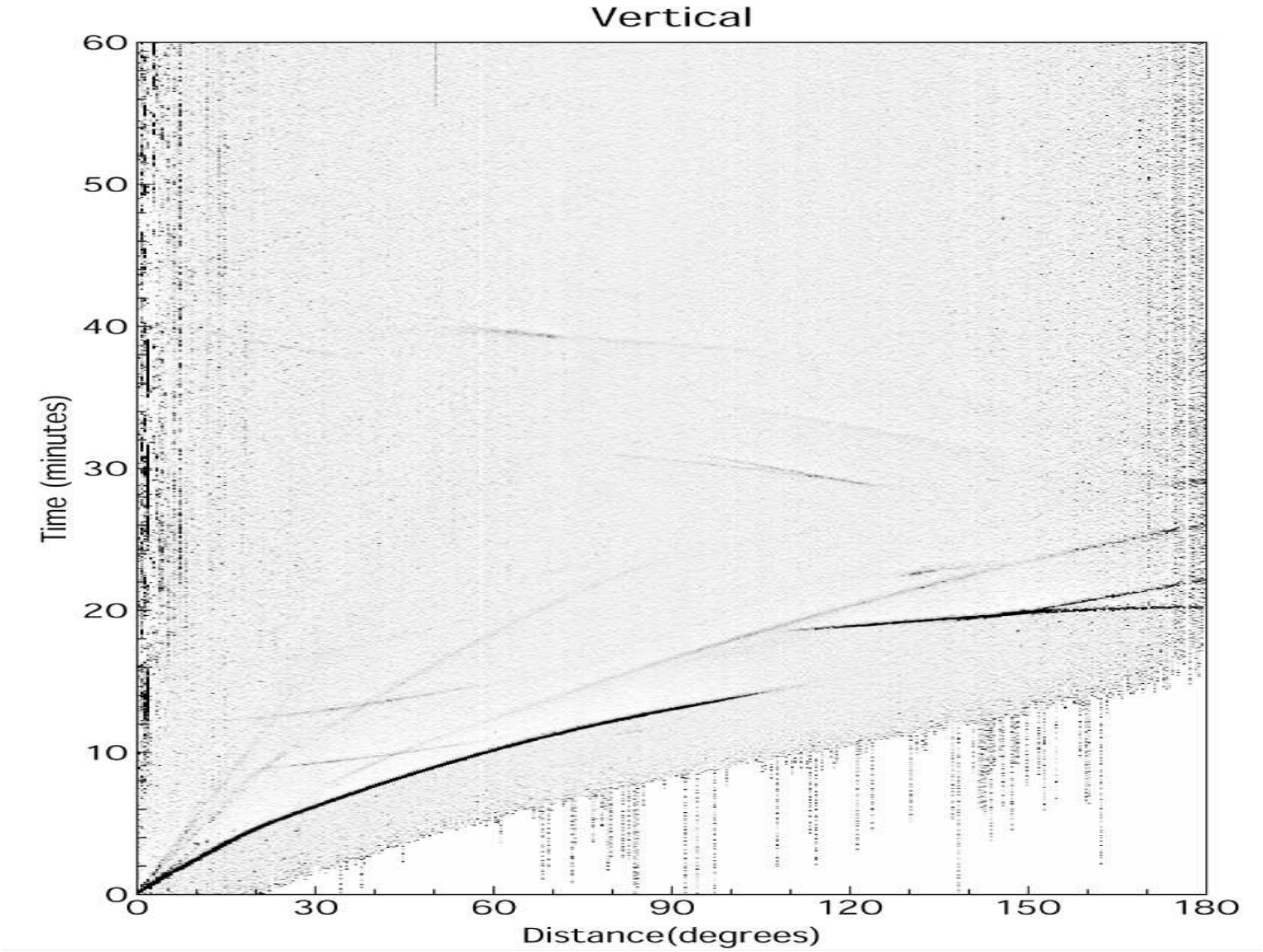

Astiz et al. (1996)

First-order discontinuities

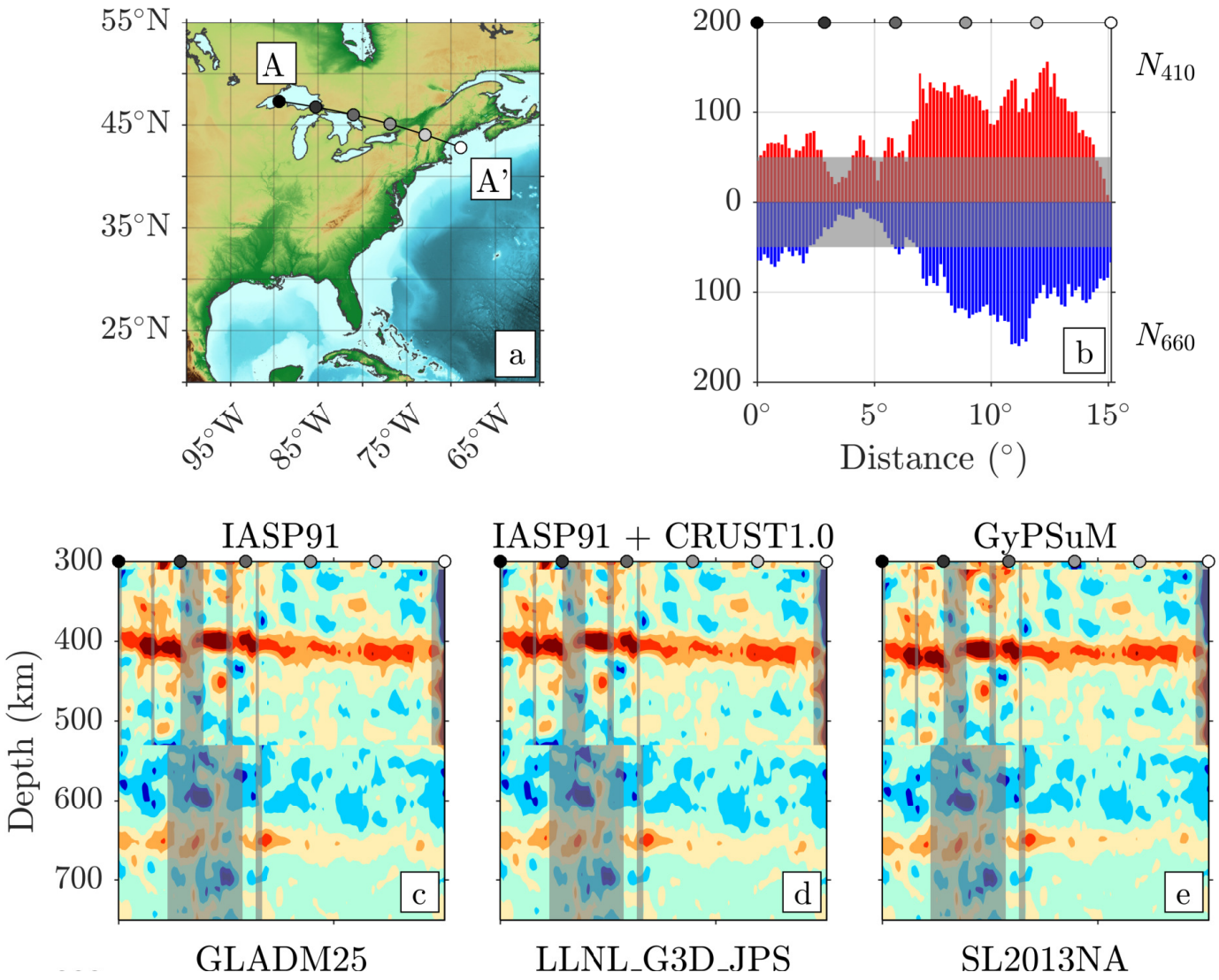

Burky et al. (2023)

Millions of travel times (noise?)

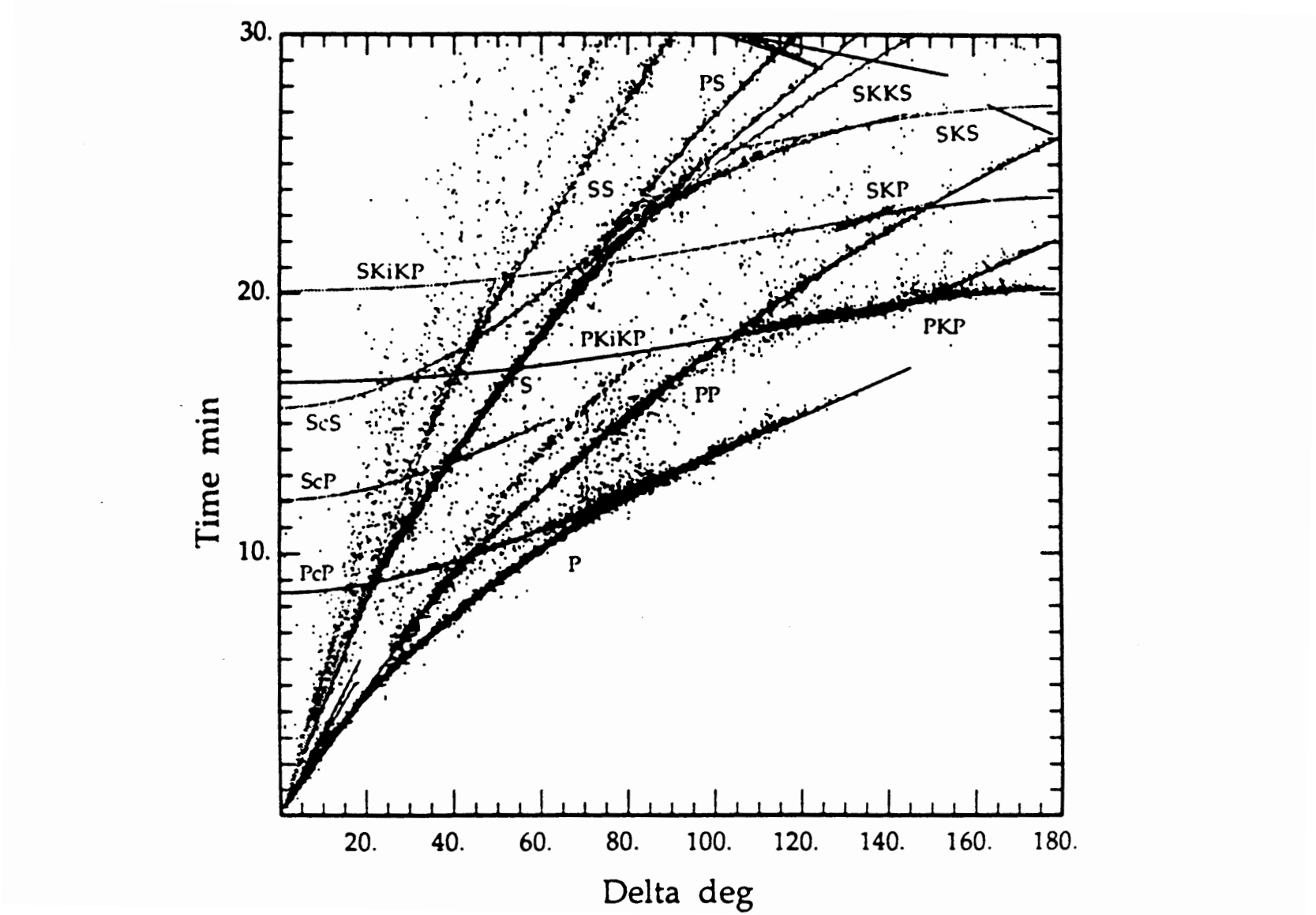

Kennett and Engdahl (1991)

Three-dimensional Earth structure

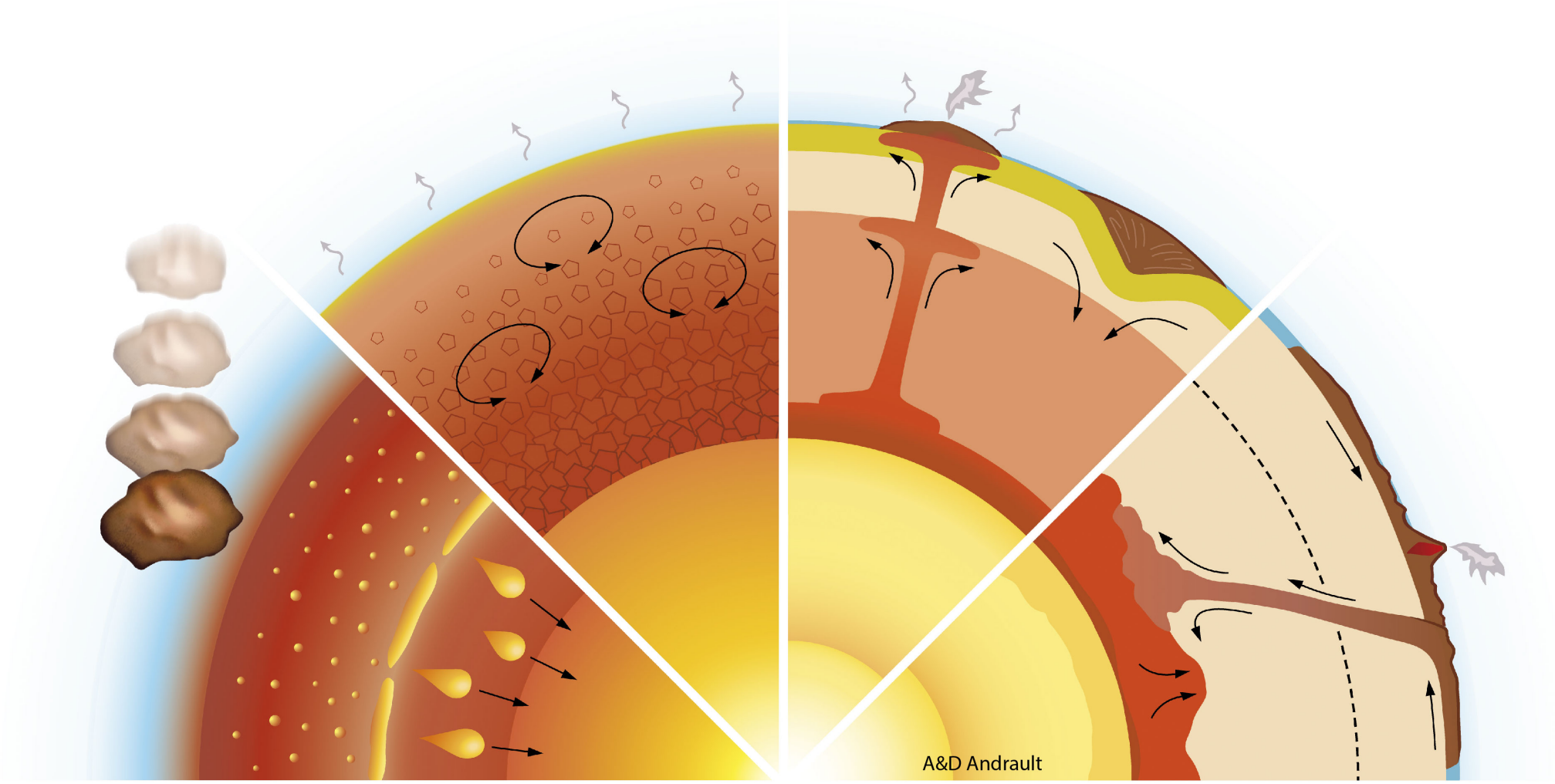

Tomography!

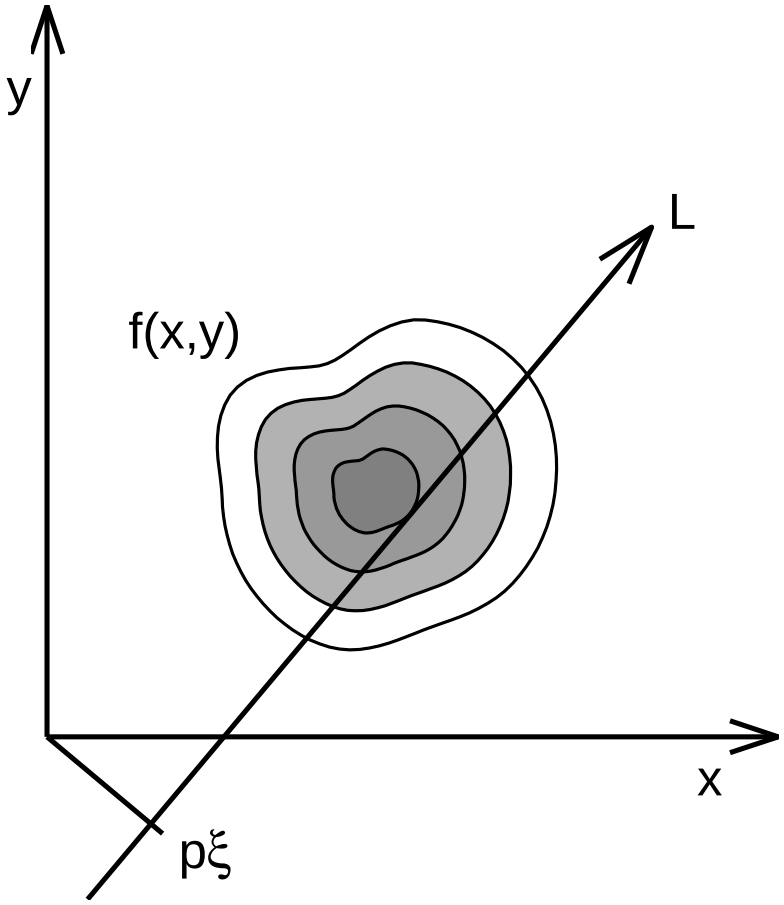

Tomography!

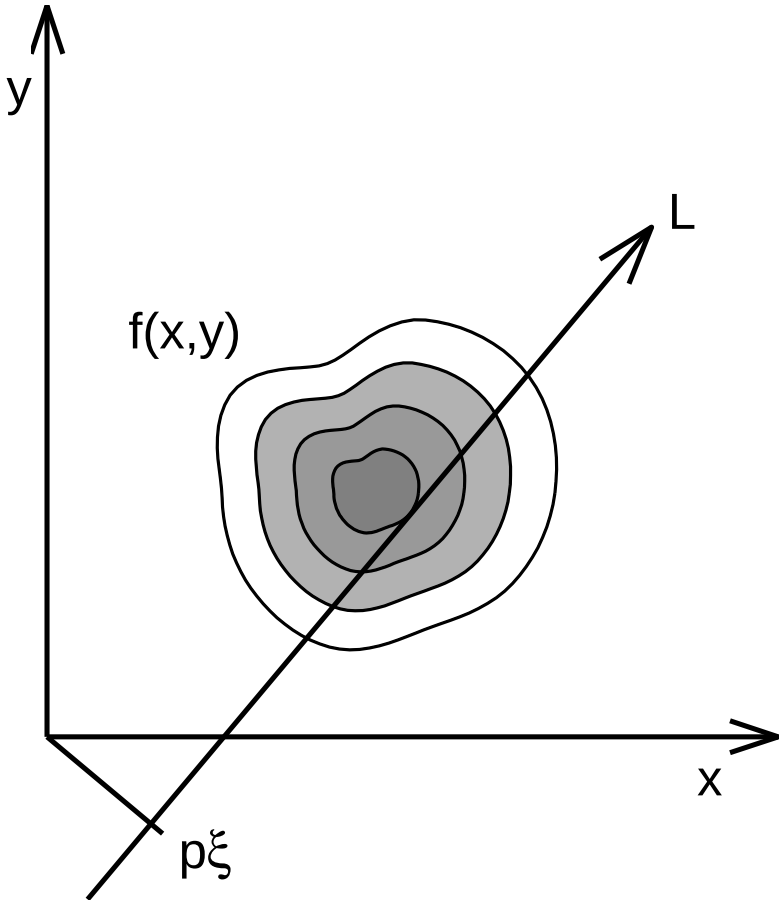

Inverting the Radon transform

$$\mathcal{R}[f](p, \boldsymbol{\xi}) = \int_L f(x, y)\, ds. \qquad (1)$$

Reconstruct the function from its projections:

given $\mathcal{R}[f](p, \boldsymbol{\xi})$, find $f(x, y)$.

Tomography!

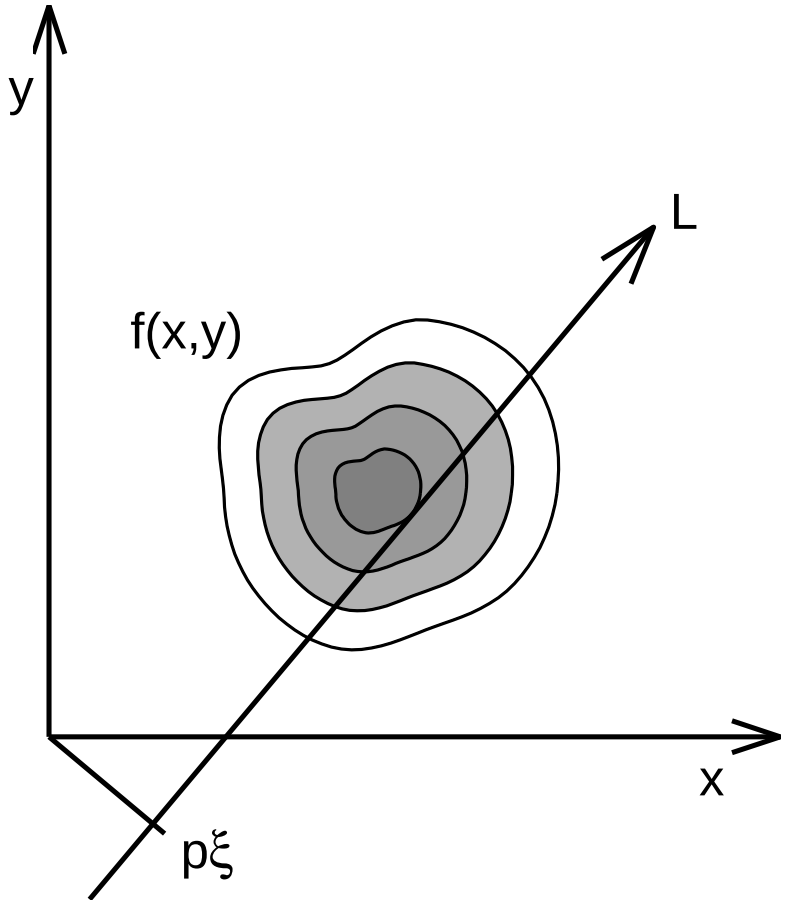

Inverting the Radon transform

$$\mathcal{R}[f](p, \boldsymbol{\xi}) = \int_L f(x, y)\, ds. \qquad (1)$$

Reconstruct the function from its projections: given $\mathcal{R}[f](p, \boldsymbol{\xi})$, find $f(x, y)$.

Radon (1917) solved to this problem, giving an expression for $\mathcal{R}^{-1}$ for straight “ray paths”.

Seismic imaging

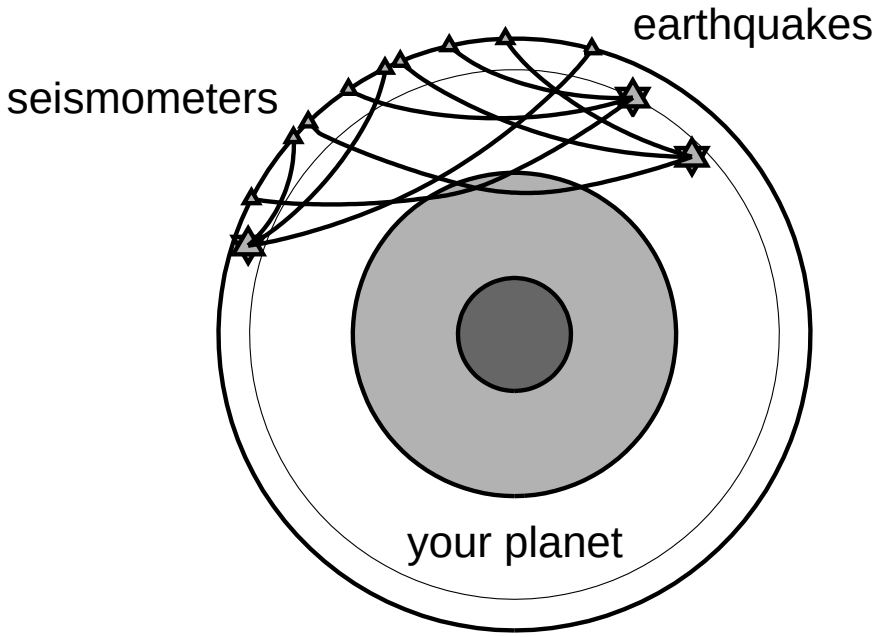

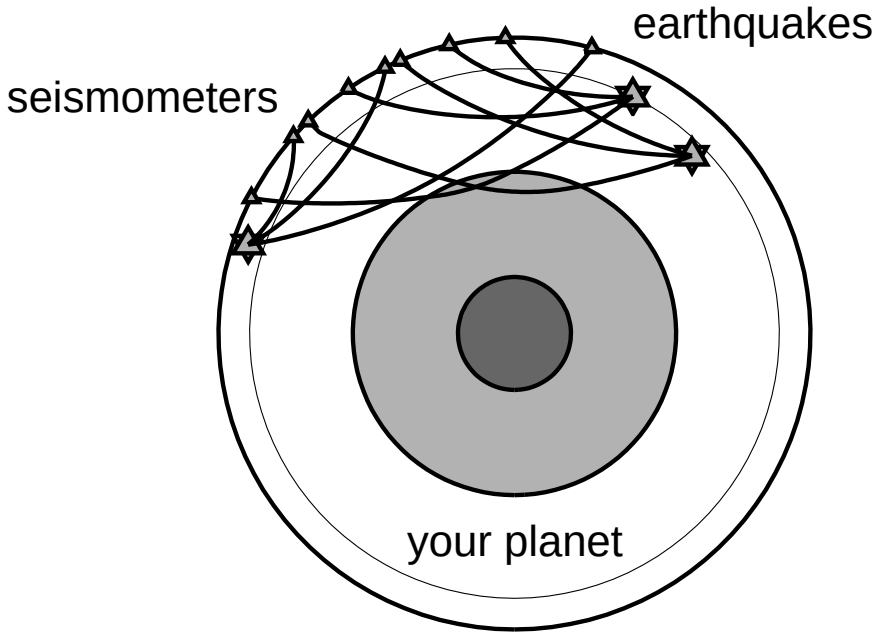

Travel-time tomography

The Earth has a heterogeneous wave-speed structure $c(\mathbf{r}) = c_0(\mathbf{r}) + \delta c(\mathbf{r})$.

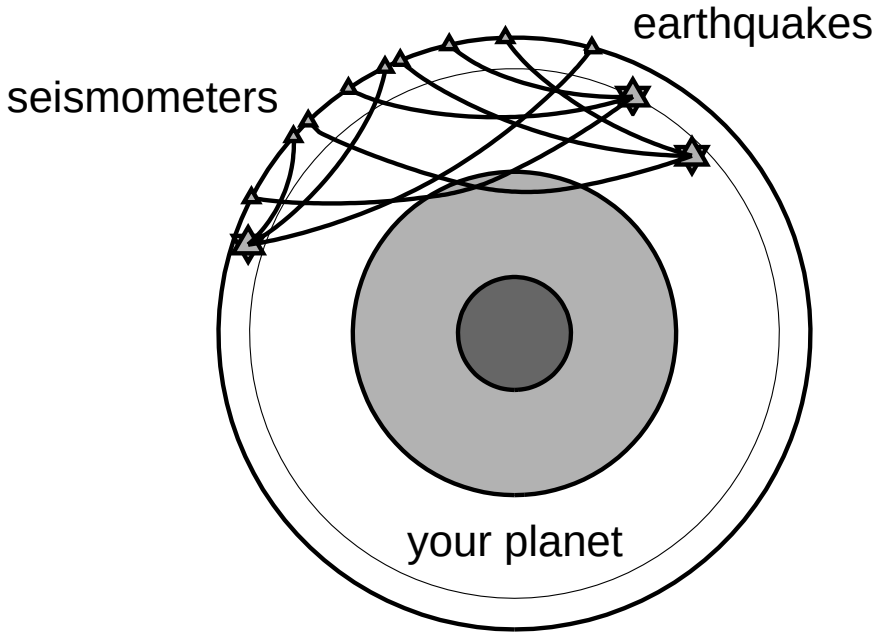

Travel-time tomography

The Earth has a heterogeneous wave-speed structure $c(\mathbf{r}) = c_0(\mathbf{r}) + \delta c(\mathbf{r})$.

Ray-theoretical travel-time anomalies are

$$\delta t \approx \int_{\text{ray}} \delta c^{-1}\, ds \approx -\int_{\text{ray}} \frac{\delta c}{c_0^2}\, ds. \quad (2)$$

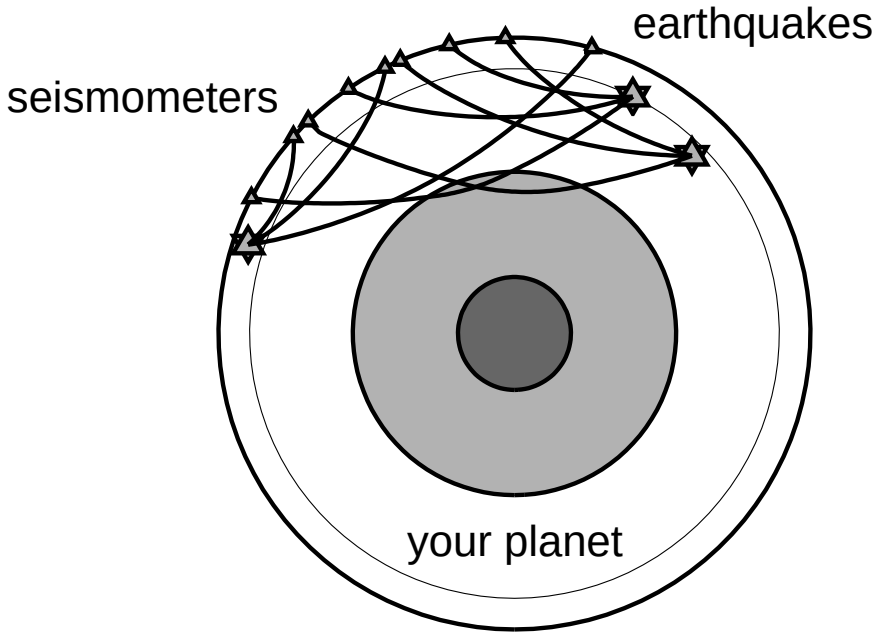

Travel-time tomography

The Earth has a heterogeneous wave-speed structure $c(\mathbf{r}) = c_0(\mathbf{r}) + \delta c(\mathbf{r})$.

Ray-theoretical travel-time anomalies are

$$\delta t \approx \int\limits_{\mathrm{ray}} \delta c^{-1}\, ds \approx -\int\limits_{\mathrm{ray}} \frac{\delta c}{c_0^2}\, ds. \quad (2)$$

Fermat's principle allows ray to be calculated in the reference model $c_0(\mathbf{r})$.

Usually, not exclusively, $c_0(\mathbf{r}) = c_0(r)$.

Fermat's principle

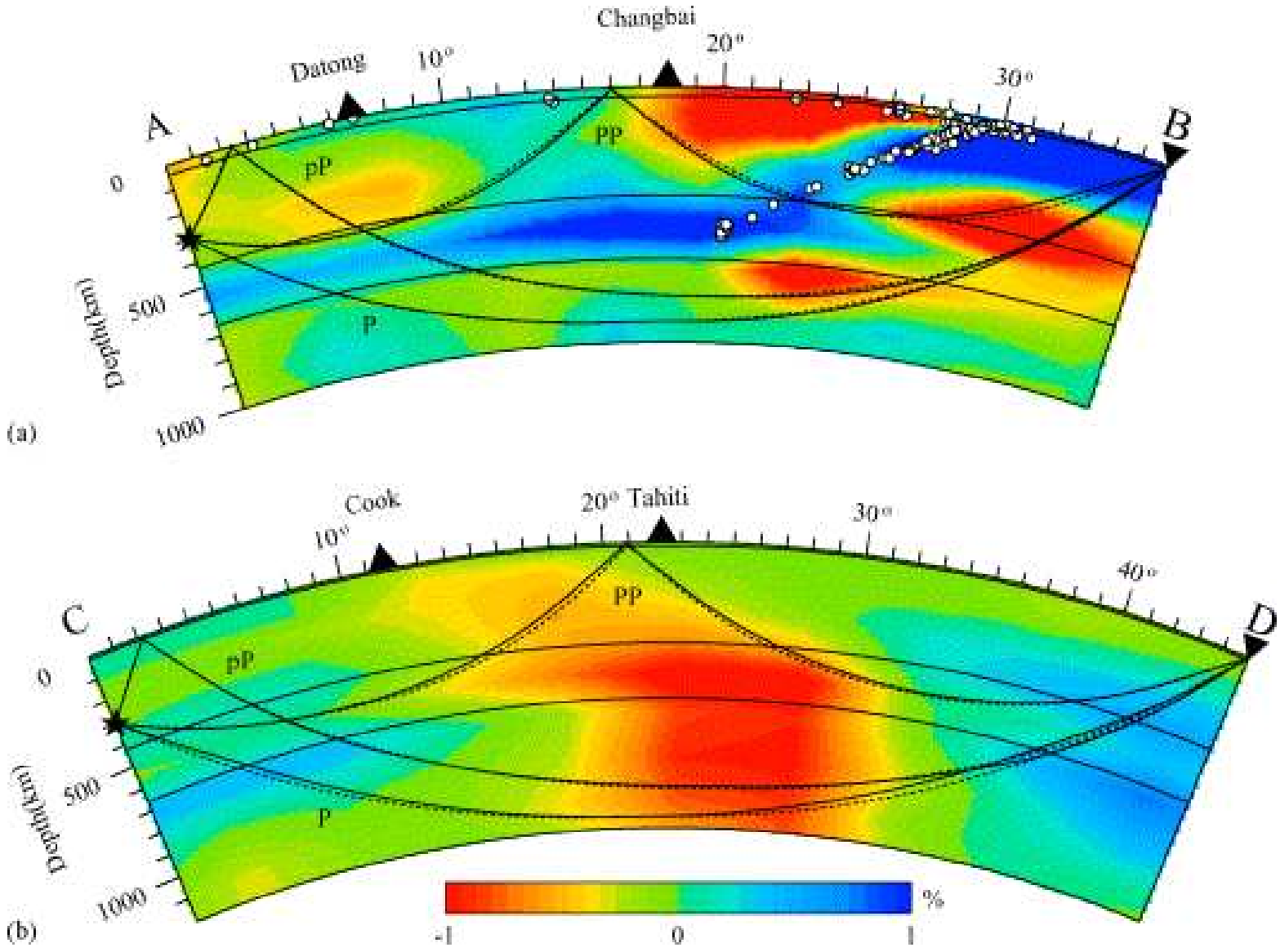

Zhao and Lei (2004)

Discretization and parameterization

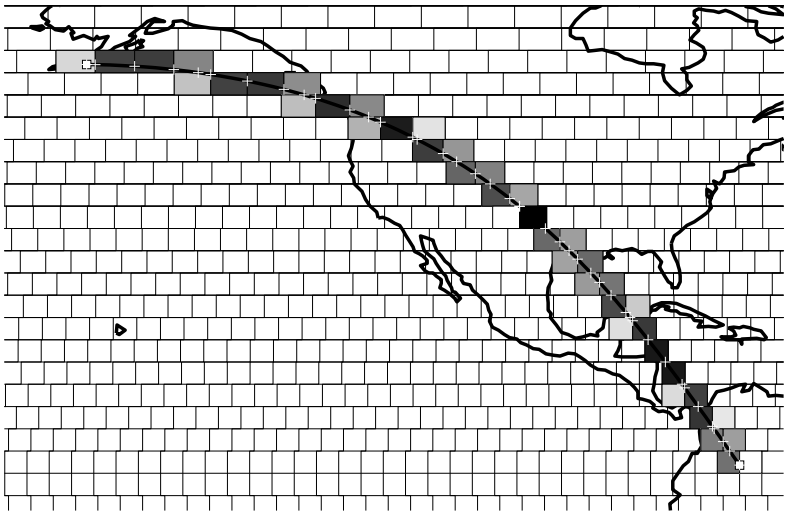

Discretization and parameterization

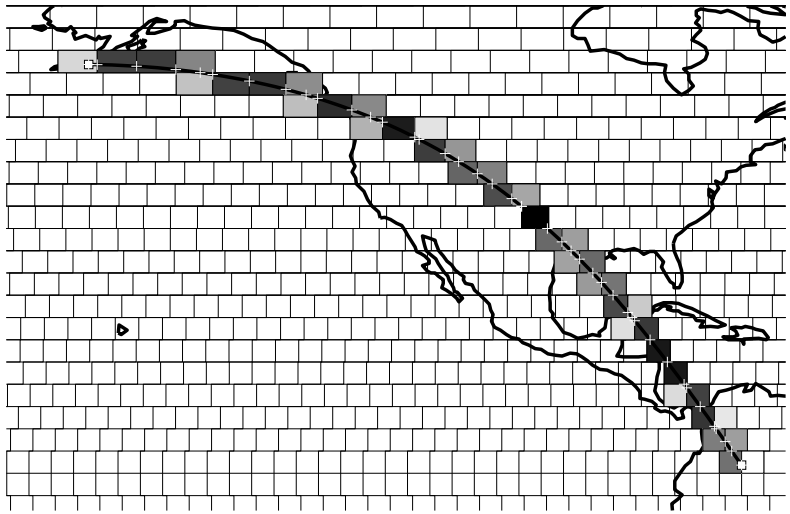

For a set of seismic rays $i = 1 \rightarrow M$, calculate the length spent in each of the $j = 1 \rightarrow N$ grid boxes in which it accumulates a proportional fraction of the total travel-time anomaly δt, discretizing (2).

Discretization and parameterization

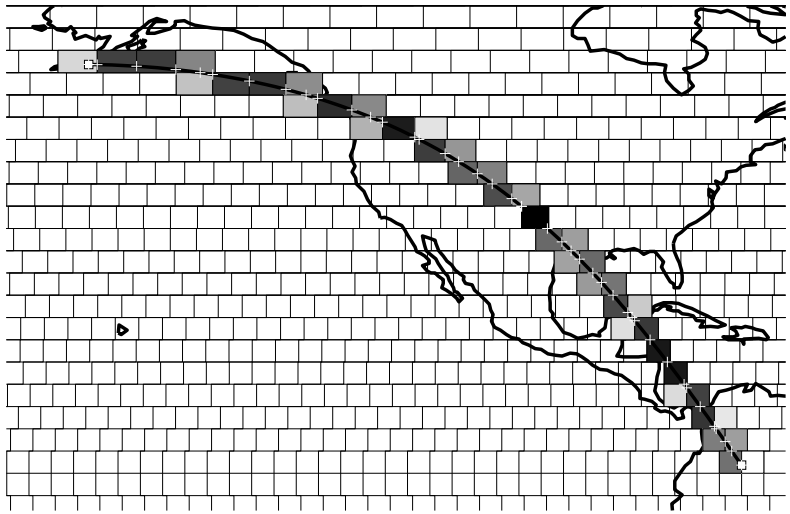

For a set of seismic rays $i = 1 \rightarrow M$, calculate the length spent in each of the $j = 1 \rightarrow N$ grid boxes in which it accumulates a proportional fraction of the total travel-time anomaly δt, discretizing (2).

$$\delta t_i = s_{ij}\, \delta c_j^{-1} \quad \text{or} \quad \boldsymbol{\delta \mathbf{t}} = \mathbf{S} \cdot \boldsymbol{\delta \mathbf{c}^{-1}} \quad \text{or indeed} \quad \mathbf{d} = \mathbf{G} \cdot \mathbf{m}$$

Discretization and parameterization

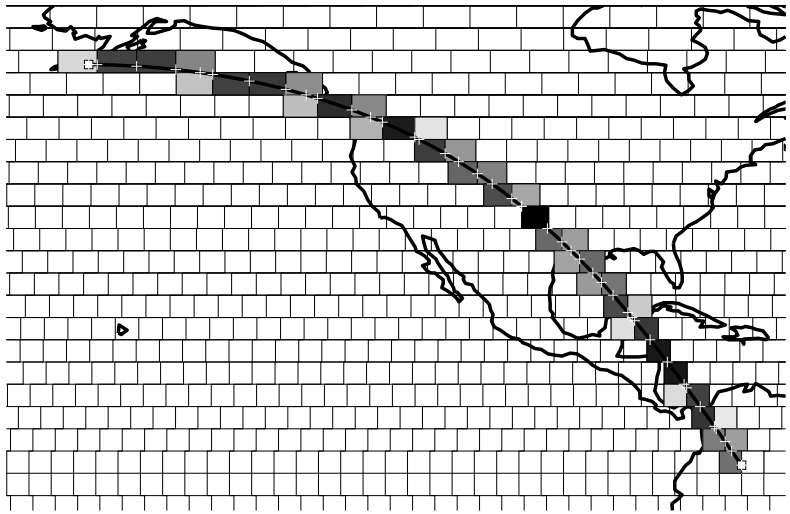

For a set of seismic rays $i = 1 \rightarrow M$, calculate the length spent in each of the $j = 1 \rightarrow N$ grid boxes in which it accumulates a proportional fraction of the total travel-time anomaly δt, discretizing (2).

$$\delta t_i = s_{ij}\, \delta c_j^{-1} \quad \text{or} \quad \boldsymbol{\delta \mathbf{t}} = \mathbf{S} \cdot \boldsymbol{\delta \mathbf{c}^{-1}} \quad \text{or indeed} \quad \mathbf{d} = \mathbf{G} \cdot \mathbf{m} \tag{3}$$

travel-time anomalies

$$\begin{bmatrix} \vdots \\ \delta t_i \\ \vdots \end{bmatrix} = \begin{bmatrix} \vdots \\ \dots \quad s_{ij} \quad \dots \\ \vdots \end{bmatrix} \times \begin{bmatrix} \vdots \\ \delta c_j^{-1} \\ \vdots \end{bmatrix}$$

slowness perturbations

(4)

tall **sensitivity matrix**

Solving the inverse problem

We have: $\mathbf{G} \cdot \mathbf{m} = \mathbf{d},$ which is **linear**.

Solving the inverse problem

We have: $\mathbf{G} \cdot \mathbf{m} = \mathbf{d}$, which is **linear**.

You think: $\mathbf{m} = \mathbf{G}^{-1} \cdot \mathbf{d}$, but we **can't invert** a non-square $M \times N$ matrix.

Solving the inverse problem

We have: $\mathbf{G} \cdot \mathbf{m} = \mathbf{d}$, which is **linear**.

You think: $\mathbf{m} = \mathbf{G}^{-1} \cdot \mathbf{d}$, but we **can't invert** a non-square $M \times N$ matrix.

You think: $\mathbf{G}^{\mathrm{T}} \cdot \mathbf{G}$ is square, let's solve $\mathbf{G}^{\mathrm{T}} \cdot \mathbf{G} \cdot \mathbf{m} = \mathbf{G}^{\mathrm{T}} \cdot \mathbf{d}$.

Solving the inverse problem

We have: $\mathbf{G} \cdot \mathbf{m} = \mathbf{d}$, which is **linear**.

You think: $\mathbf{m} = \mathbf{G}^{-1} \cdot \mathbf{d}$, but we **can't invert** a non-square $M \times N$ matrix.

You think: $\mathbf{G}^{\mathrm{T}} \cdot \mathbf{G}$ is square, let's solve $\mathbf{G}^{\mathrm{T}} \cdot \mathbf{G} \cdot \mathbf{m} = \mathbf{G}^{\mathrm{T}} \cdot \mathbf{d}$.

You try: $\mathbf{m} = (\mathbf{G}^{\mathrm{T}} \cdot \mathbf{G})^{-1} \cdot \mathbf{G}^{\mathrm{T}} \cdot \mathbf{d}$.

Solving the inverse problem

We have:	$\mathbf{G} \cdot \mathbf{m} = \mathbf{d}$,	which is **linear**.
You think:	$\mathbf{m} = \mathbf{G}^{-1} \cdot \mathbf{d}$,	but we **can't invert** a non-square $M \times N$ matrix.
You think:	$\mathbf{G}^{\mathrm{T}} \cdot \mathbf{G}$	is square, let's solve $\mathbf{G}^{\mathrm{T}} \cdot \mathbf{G} \cdot \mathbf{m} = \mathbf{G}^{\mathrm{T}} \cdot \mathbf{d}$.
You try:	$\mathbf{m} = (\mathbf{G}^{\mathrm{T}} \cdot \mathbf{G})^{-1} \cdot \mathbf{G}^{\mathrm{T}} \cdot \mathbf{d}$.	
Alas!	$\mathbf{G}^{\mathrm{T}} \cdot \mathbf{G}$	may be singular, ill-conditioned, under/over-determined, have (near-)zero eigenvalues, and thus be **not-invertible**. We need **regularization**.

Solving the inverse problem

We have: $\mathbf{G} \cdot \mathbf{m} = \mathbf{d}$, which is **linear**.

You think: $\mathbf{m} = \mathbf{G}^{-1} \cdot \mathbf{d}$, but we **can't invert** a non-square $M \times N$ matrix.

You think: $\mathbf{G}^{\mathrm{T}} \cdot \mathbf{G}$ is square, let's solve $\mathbf{G}^{\mathrm{T}} \cdot \mathbf{G} \cdot \mathbf{m} = \mathbf{G}^{\mathrm{T}} \cdot \mathbf{d}$.

You try: $\mathbf{m} = (\mathbf{G}^{\mathrm{T}} \cdot \mathbf{G})^{-1} \cdot \mathbf{G}^{\mathrm{T}} \cdot \mathbf{d}$.

Alas! $\mathbf{G}^{\mathrm{T}} \cdot \mathbf{G}$ may be singular, ill-conditioned, under/over-determined, have (near-)zero eigenvalues, and thus be **not-invertible**. We need **regularization**.

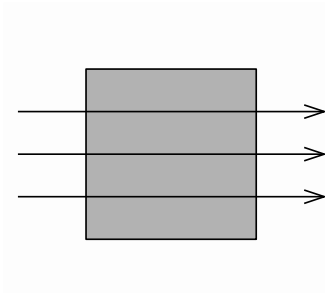

over-determined, M>N

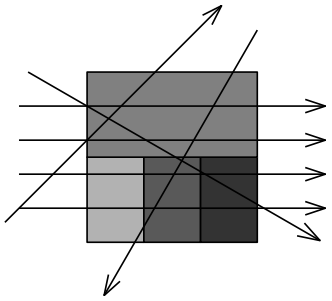

mixed-determined

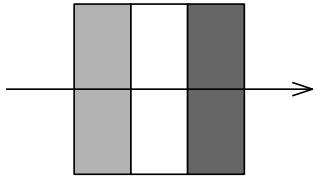

under-determined, M<N

Menke (1989); *Aster et al.* (2005)

Global models – I

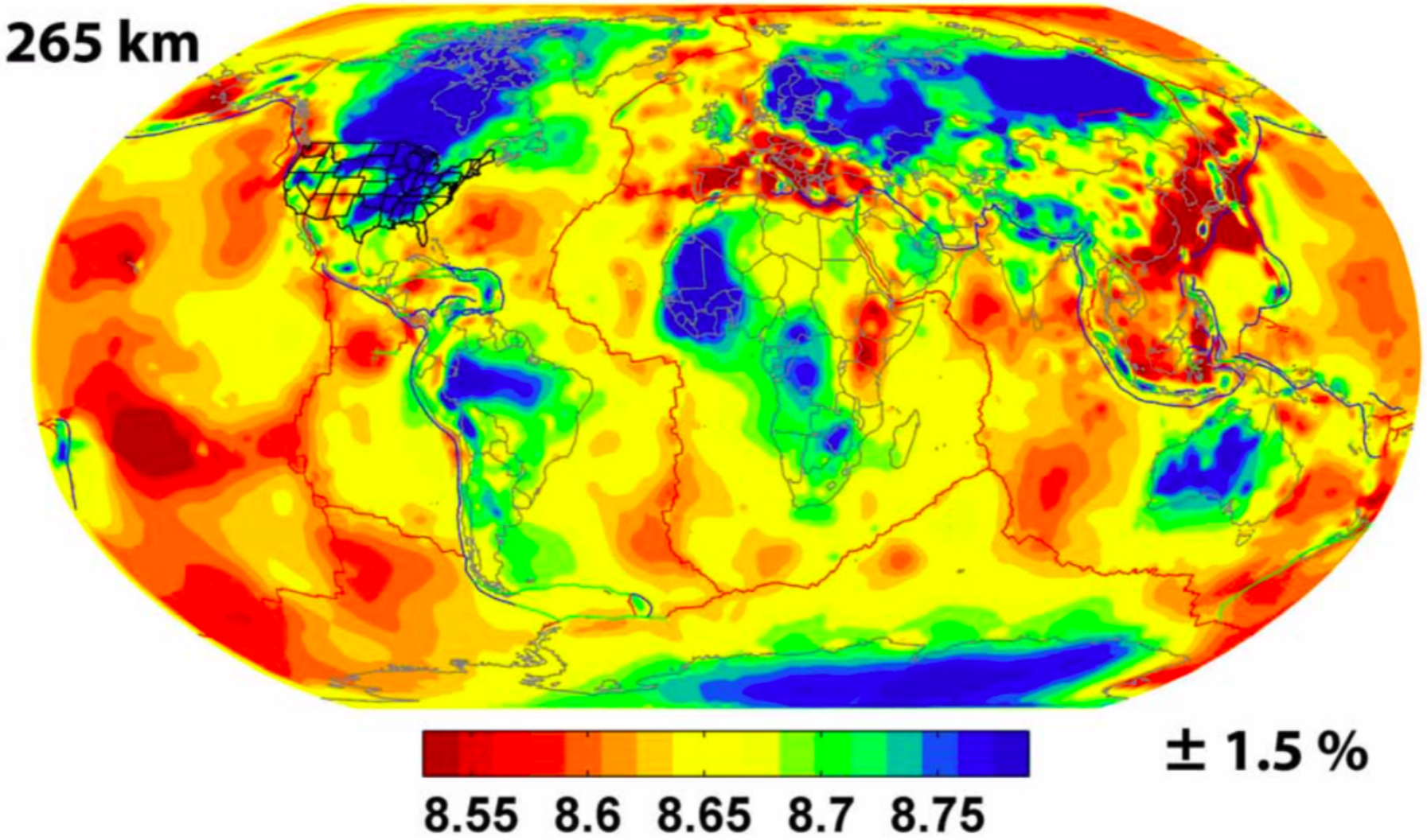

Simmons et al. (2012)

Sensitivity: Wavefront healing

After discretization, parameterization, and regularization, every infinite-frequency, "optical", **geometrical ray** illuminates a **"fat tube"** in the model space.

Sensitivity: Wavefront healing

After discretization, parameterization, and regularization, every infinite-frequency, "optical", **geometrical ray** illuminates a **"fat tube"** in the model space.

But the **basic premise** — that a velocity anomaly sensed anywhere along the ray shows up as a travel-time anomaly at the receiver — is **wrong**. Wavefronts **heal**.

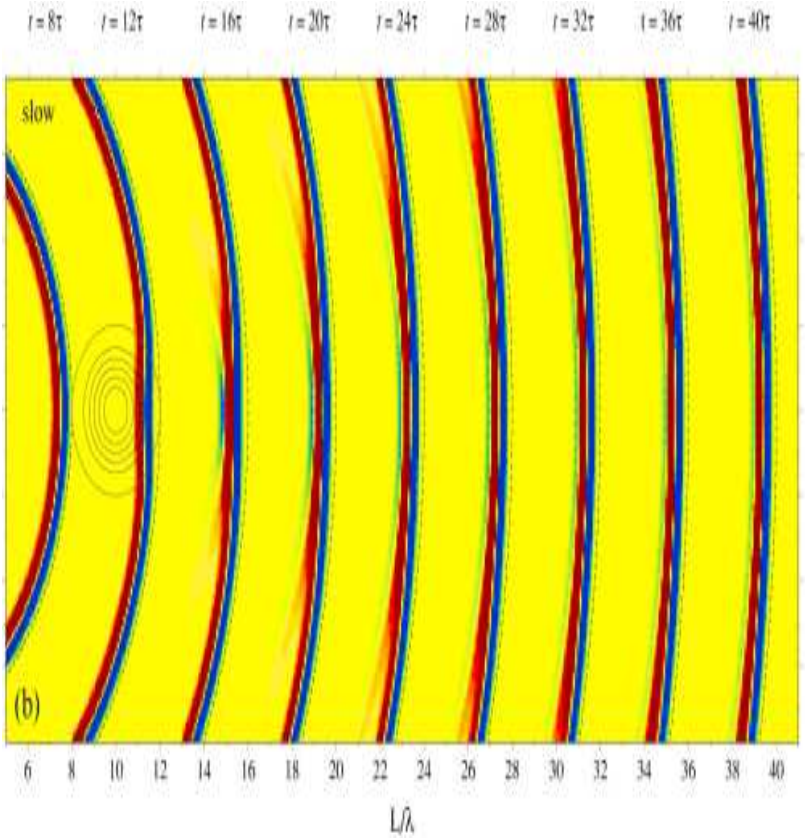

(*Hung et al.*, 2001)

Sensitivity: Infinite and finite frequencies

What we did is only true when the wave is of an **infinitely high frequency**:

$$\delta t \approx \int_{\text{ray}} \left[-c_0^{-1}\right] \left(\frac{\delta c}{c_0}\right) \, ds. \tag{5}$$

Sensitivity: Infinite and finite frequencies

What we did is only true when the wave is of an **infinitely high frequency**:

$$\delta t \approx \int_{\text{ray}} \left[-c_0^{-1}\right] \left(\frac{\delta c}{c_0}\right) \, ds. \tag{5}$$

Only at $\omega \rightarrow \infty$ is the **sensitivity kernel** of the measurement δt to the model perturbation $\delta c / c_0$ given by c_0^{-1} exclusively *on the geometrical ray path*.

Sensitivity: Infinite and finite frequencies

What we did is only true when the wave is of an **infinitely high frequency**:

$$\delta t \approx \int_{\text{ray}} \left[-c_0^{-1}\right] \left(\frac{\delta c}{c_0}\right) \, ds. \tag{5}$$

Only at $\omega \to \infty$ is the **sensitivity kernel** of the measurement δt to the model perturbation $\delta c / c_0$ given by c_0^{-1} exclusively *on the geometrical ray path*.

In reality, waves have a **finite frequency**, and measurements are at many different frequencies at that. The wave "feels" *off the ray*.

$$\delta t \approx \iiint_{\text{Earth}} K_{\delta t} \left(\frac{\delta c}{c_0}\right) \, dV. \tag{6}$$

Finding $K_{\delta t}$, a **3D Fréchet kernel**, is the name of the game.

What are we measuring?

A **finite-frequency travel-time anomaly** is the time shift given by maximizing the **cross-correlation** of an observed seismogram, $u(t) = u_0(t) + \delta u(t)$, with the synthetic wavefield, $u_0(t)$, computed in the reference model $c_0 = (\rho_0, \mathbf{C}_0)$:

$$\delta t = \arg\max \int_{t_1}^{t_2} u(t - \delta t)\, u_0(t)\, dt. \tag{7}$$

What are we measuring?

A **finite-frequency travel-time anomaly** is the time shift given by maximizing the **cross-correlation** of an observed seismogram, $u(t) = u_0(t) + \delta u(t)$, with the synthetic wavefield, $u_0(t)$, computed in the reference model $c_0 = (\rho_0, \mathbf{C}_0)$:

$$\delta t = \arg\max \int_{t_1}^{t_2} u(t - \delta t)\, u_0(t)\, dt. \tag{7}$$

The waveform perturbation $\delta u(t)$ comes from perturbations in the **Earth model**:

$$\rho_0 \to \rho_0 + \delta\rho \quad \text{and} \quad \mathbf{C_0} \to \mathbf{C_0} + \delta\mathbf{C}, \tag{8}$$

$$\mathbf{u_0} \to \mathbf{u_0} + \delta\mathbf{u}, \tag{9}$$

where ρ is density, $\mathbf{C}$ the elastic tensor, and linearization the **Born approximation**.

What are we measuring?

A **finite-frequency travel-time anomaly** is the time shift given by maximizing the **cross-correlation** of an observed seismogram, $u(t) = u_0(t) + \delta u(t)$, with the synthetic wavefield, $u_0(t)$, computed in the reference model $c_0 = (\rho_0, \mathbf{C}_0)$:

$$\delta t = \arg\max \int_{t_1}^{t_2} u(t - \delta t)\, u_0(t)\, dt. \tag{7}$$

The waveform perturbation $\delta u(t)$ comes from perturbations in the **Earth model**:

$$\rho_0 \rightarrow \rho_0 + \delta\rho \quad \text{and} \quad \mathbf{C_0} \rightarrow \mathbf{C_0} + \delta\mathbf{C}, \tag{8}$$

$$\mathbf{u_0} \rightarrow \mathbf{u_0} + \delta\mathbf{u}, \tag{9}$$

where ρ is density, $\mathbf{C}$ the elastic tensor, and linearization the **Born approximation**. The **seismogram** $u(t)$ is any one component (vertical, radial, tangential) of the **wavefield** $\mathbf{u}(\mathbf{r}, \mathbf{t})$ measured at one particular location (the seismometer).

Two questions (only one multiple choice)

Question 1

Two questions (only one multiple choice)

Question 1

How does the measurement δt depend on the waveform perturbation δu?

There is only one answer, and it has been known for a long time:

$$\delta t = \frac{\int_{t_1}^{t_2} \dot{u}_0(t)\, \delta u(t)\, dt}{\int_{t_1}^{t_2} \ddot{u}_0(t)\, u_0(t)\, dt} = \iiint_{\text{Earth}} K_c^{\delta t} \left(\frac{\delta c}{c_0} \right) dV. \tag{10}$$

Question 2

Two questions (only one multiple choice)

Question 1

How does the measurement δt depend on the waveform perturbation δu?

There is only one answer, and it has been known for a long time:

$$\delta t = \frac{\int_{t_1}^{t_2} \dot{u}_0(t)\, \delta u(t)\, dt}{\int_{t_1}^{t_2} \ddot{u}_0(t)\, u_0(t)\, dt} = \iiint_{\text{Earth}} K_c^{\delta t} \left(\frac{\delta c}{c_0} \right) dV. \tag{10}$$

Question 2

How does the waveform perturbation $\delta u(t)$ depend on $\delta \rho$ and $\delta \mathbf{C}$ of the Earth?

The answer depends on *physical* and *numerical* approximations.

This time there are several approaches, each with its own advantages.

Luo and Schuster (1991); *Zhao and Jordan* (1998); *Marquering et al.* (1999); *Dahlen et al.* (2000); *Zhao et al.* (2000)

Fourth approach to calculate δu

The paraxial approximation. Trace only the **geometrical ray**; expand travel-time surface about it; only consider **like-type scattering** in the vicinity of the central ray.

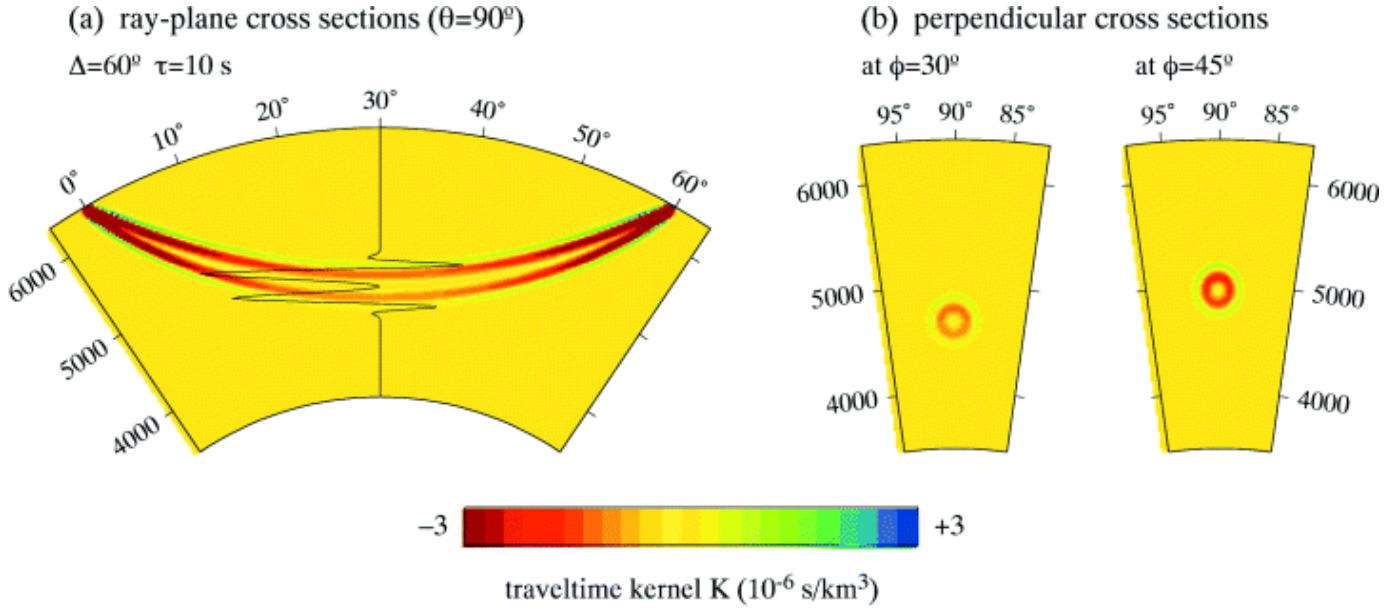

Fourth approach to calculate δu

The paraxial approximation. Trace only the **geometrical ray**; expand travel-time surface about it; only consider **like-type scattering** in the vicinity of the central ray.

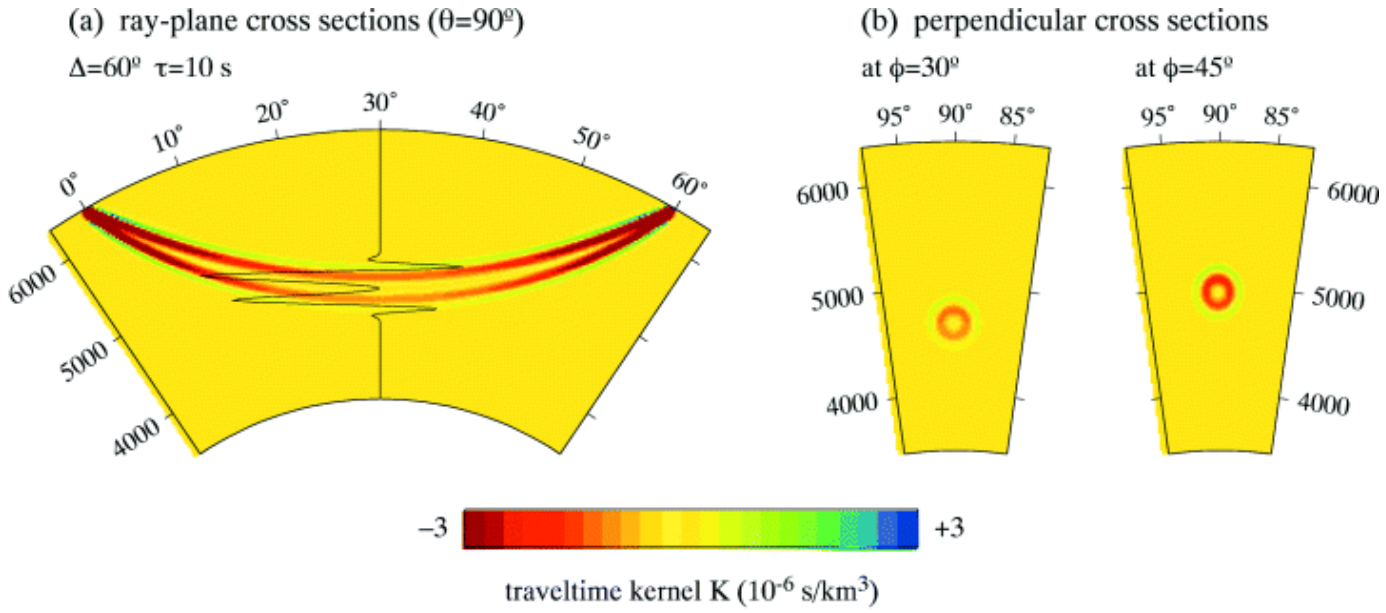

This is **much more efficient** than the previous three methods, but it breaks down somewhat earlier. However, the approximations are justifiable for common phases such as *P*, *PcP*, *PP*, *S*, *ScS*, *SS*, between 30° and 90° distance.

Dahlen et al. (2000); *Hung et al.* (2000); *Yoshizawa and Kennett* (2002)

Global models – II

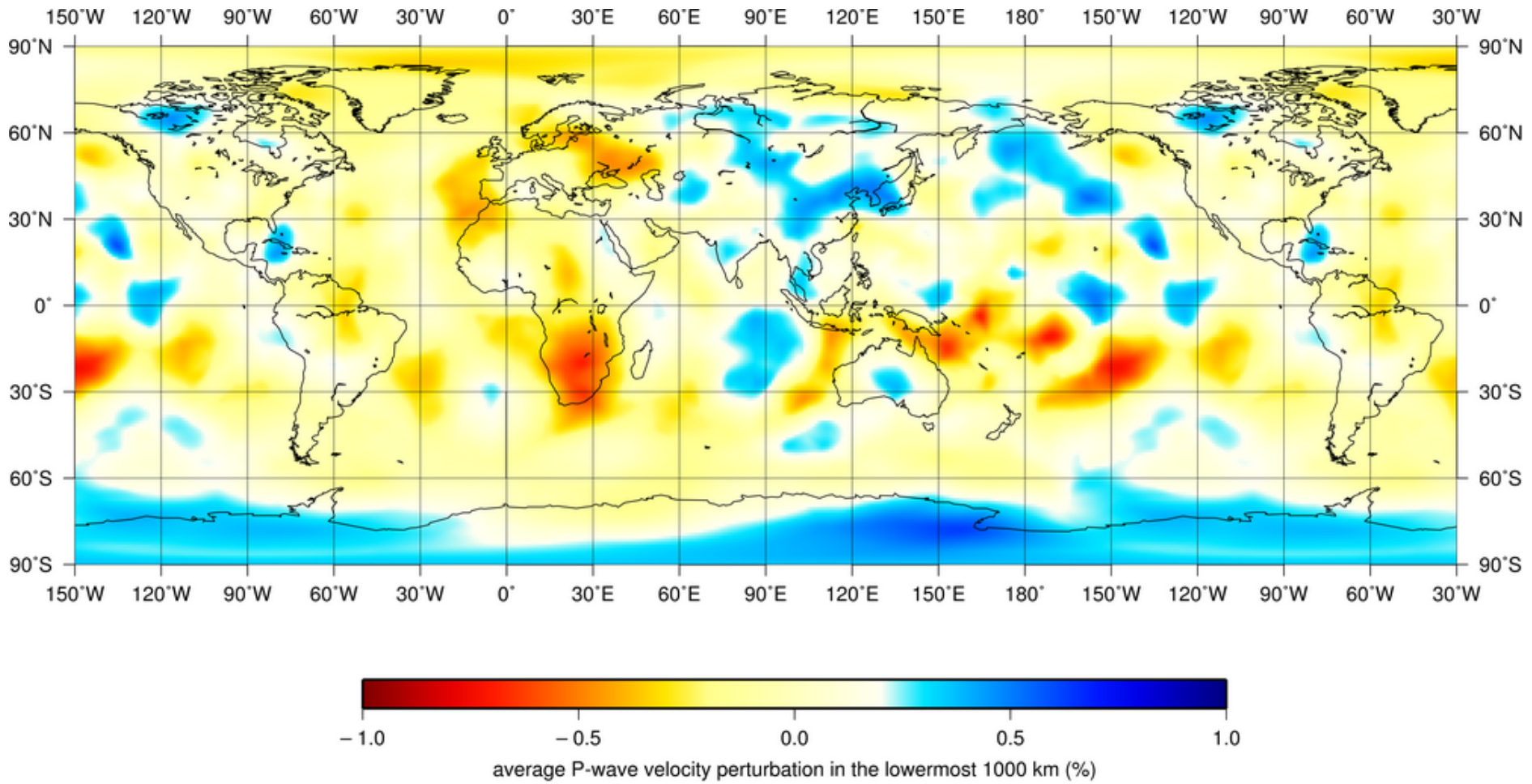

Montelli et al. (2004)

The spectral-element method

The most powerful comprehensive contemporary **grid-based method** to produce **synthetic seismograms** in **realistic** 3D media (e.g. self-gravitating, rotating, anisotropic, attenuative, heterogeneous Earth models).

The spectral-element method

The most powerful comprehensive contemporary **grid-based method** to produce **synthetic seismograms** in **realistic** 3D media (e.g. self-gravitating, rotating, anisotropic, attenuative, heterogeneous Earth models).

Combines the **geometrical flexibility** of the finite-element method with the **exponential convergence** and **weak numerical dispersion** of spectral methods.

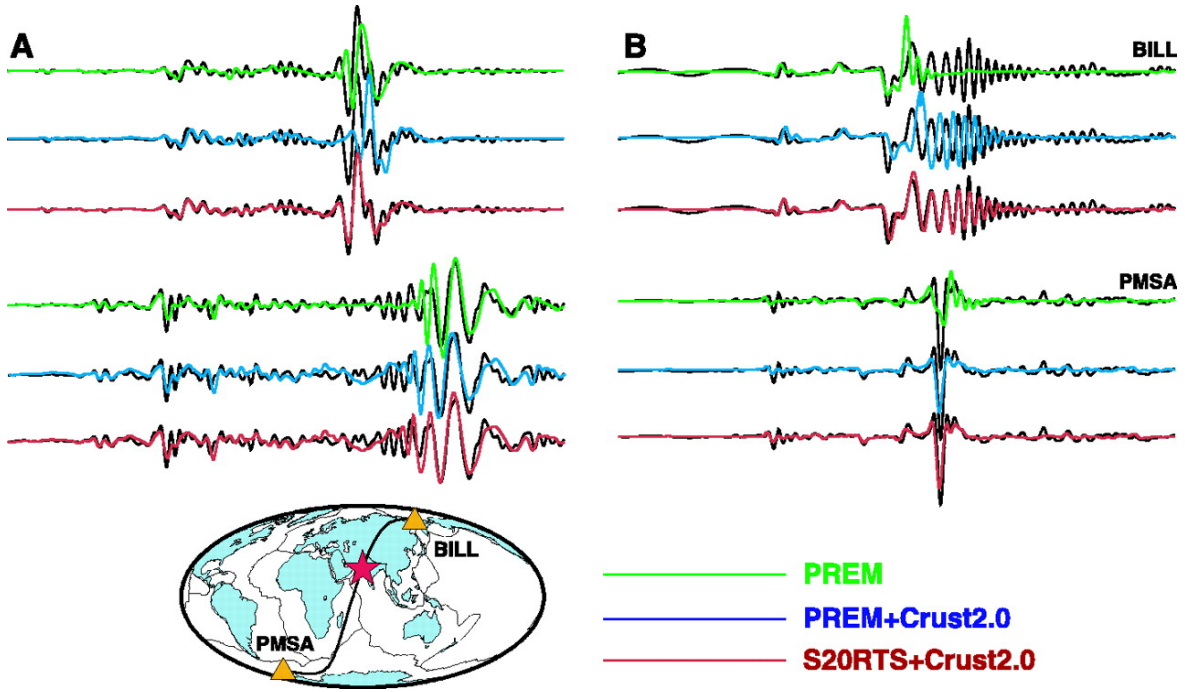

Komatitsch and Vilotte (1998); *Komatitsch and Tromp* (1999, 2002a,b); *Komatitsch et al.* (2002); *Fournier et al.* (2004)

Forward modeling using SPECFEM3D_GLOBE

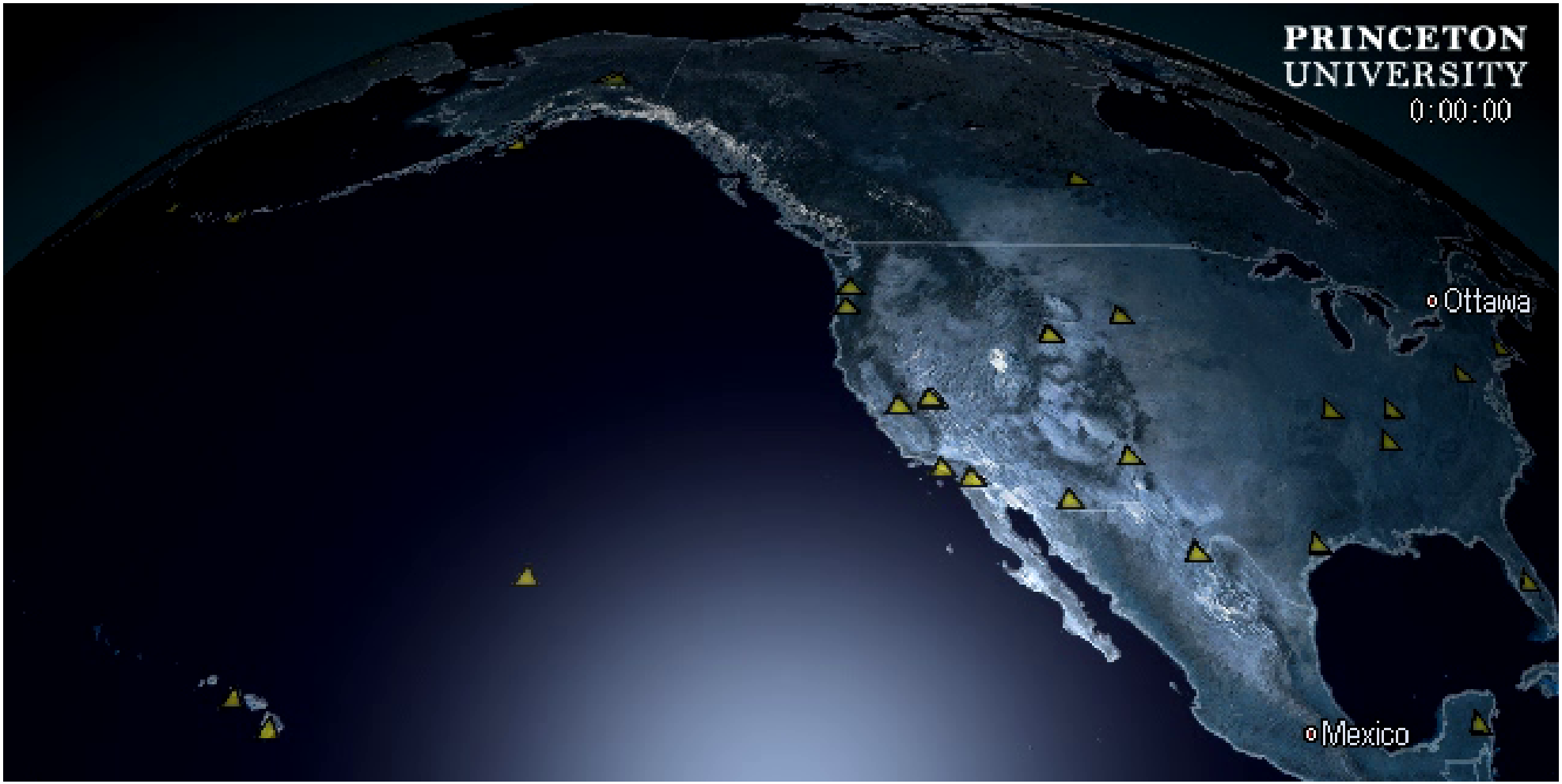

Forward modeling using SPECFEM3D_GLOBE

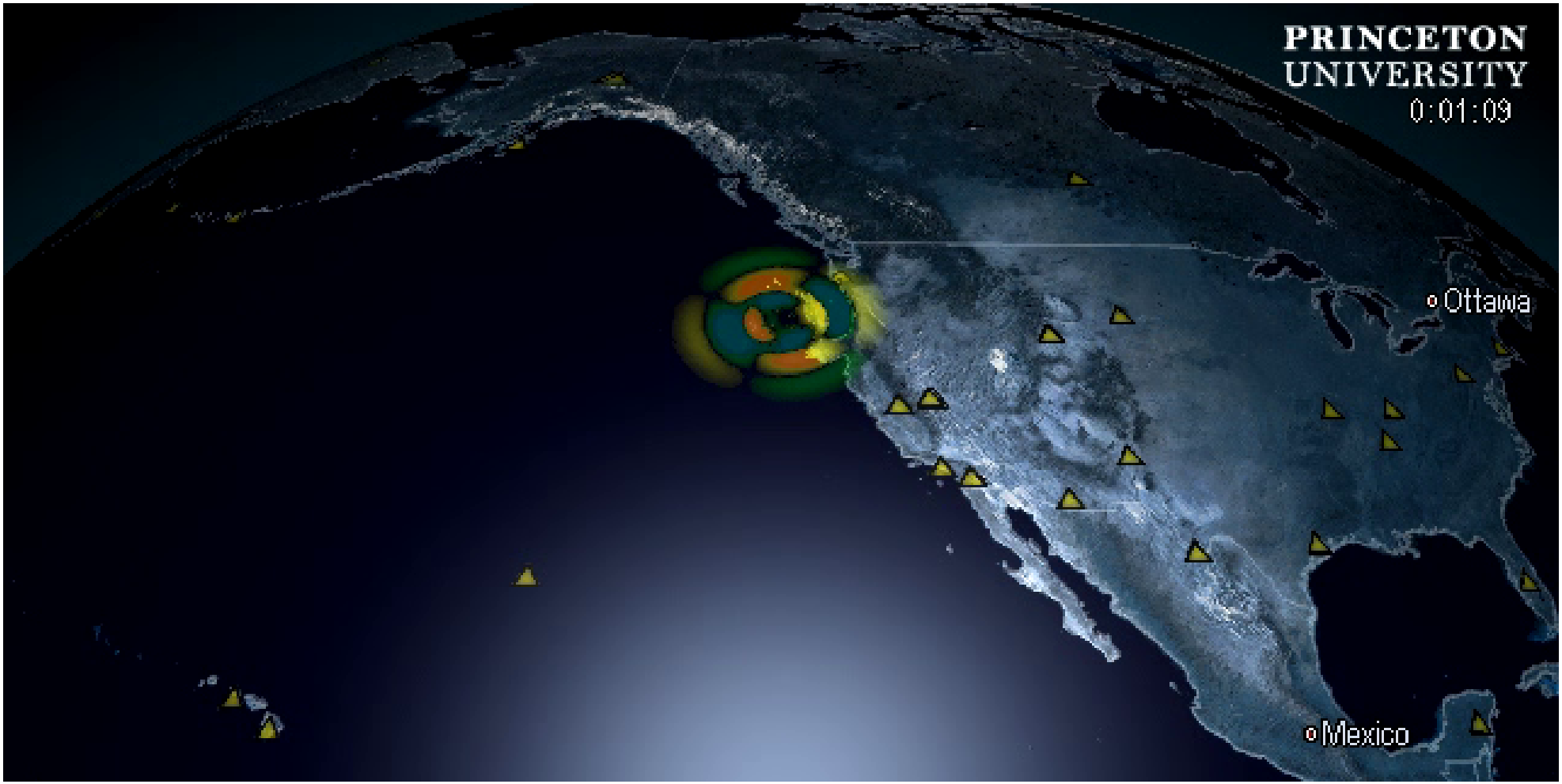

Forward modeling using SPECFEM3D_GLOBE

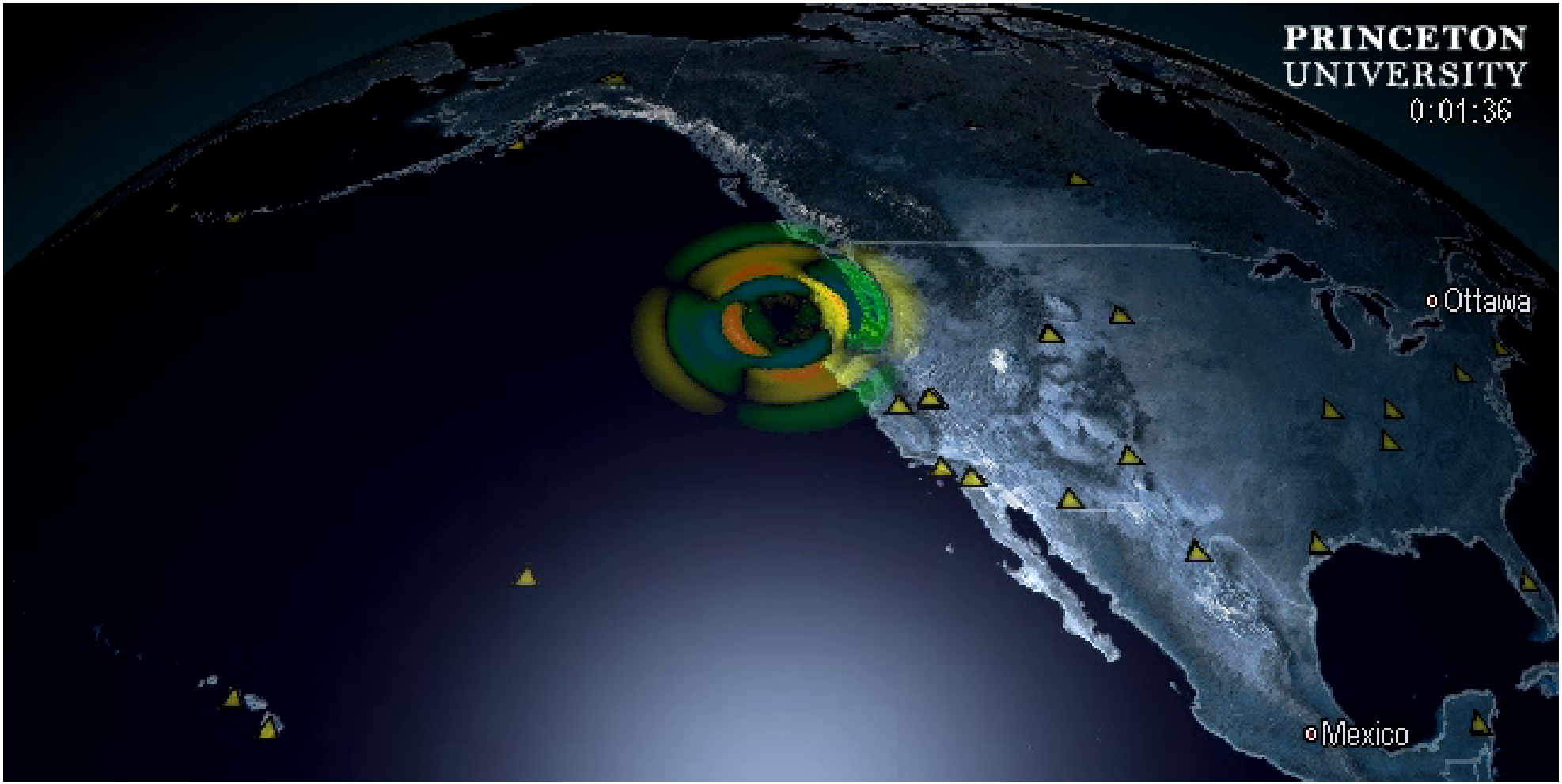

Forward modeling using SPECFEM3D_GLOBE

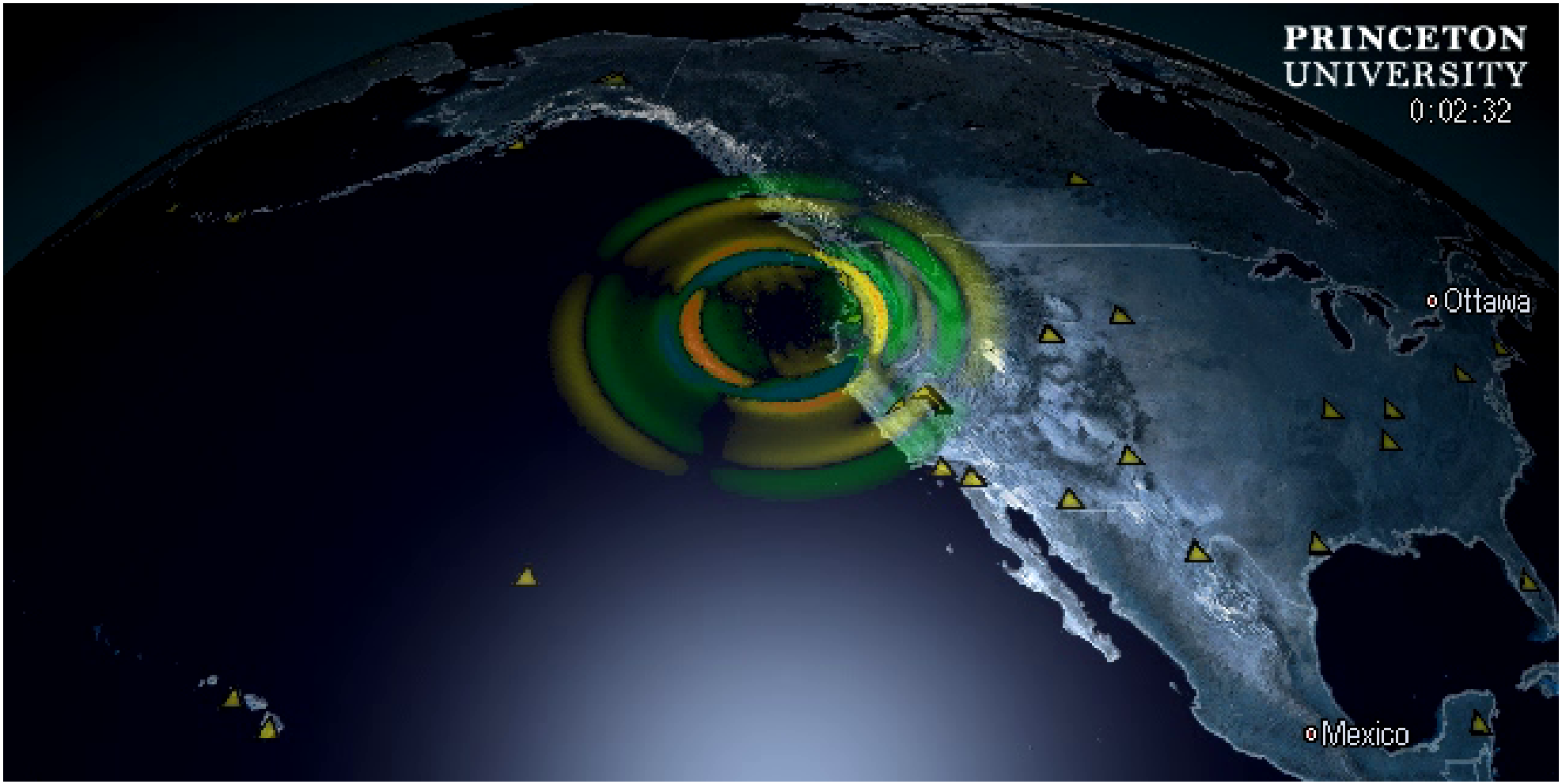

Forward modeling using SPECFEM3D_GLOBE

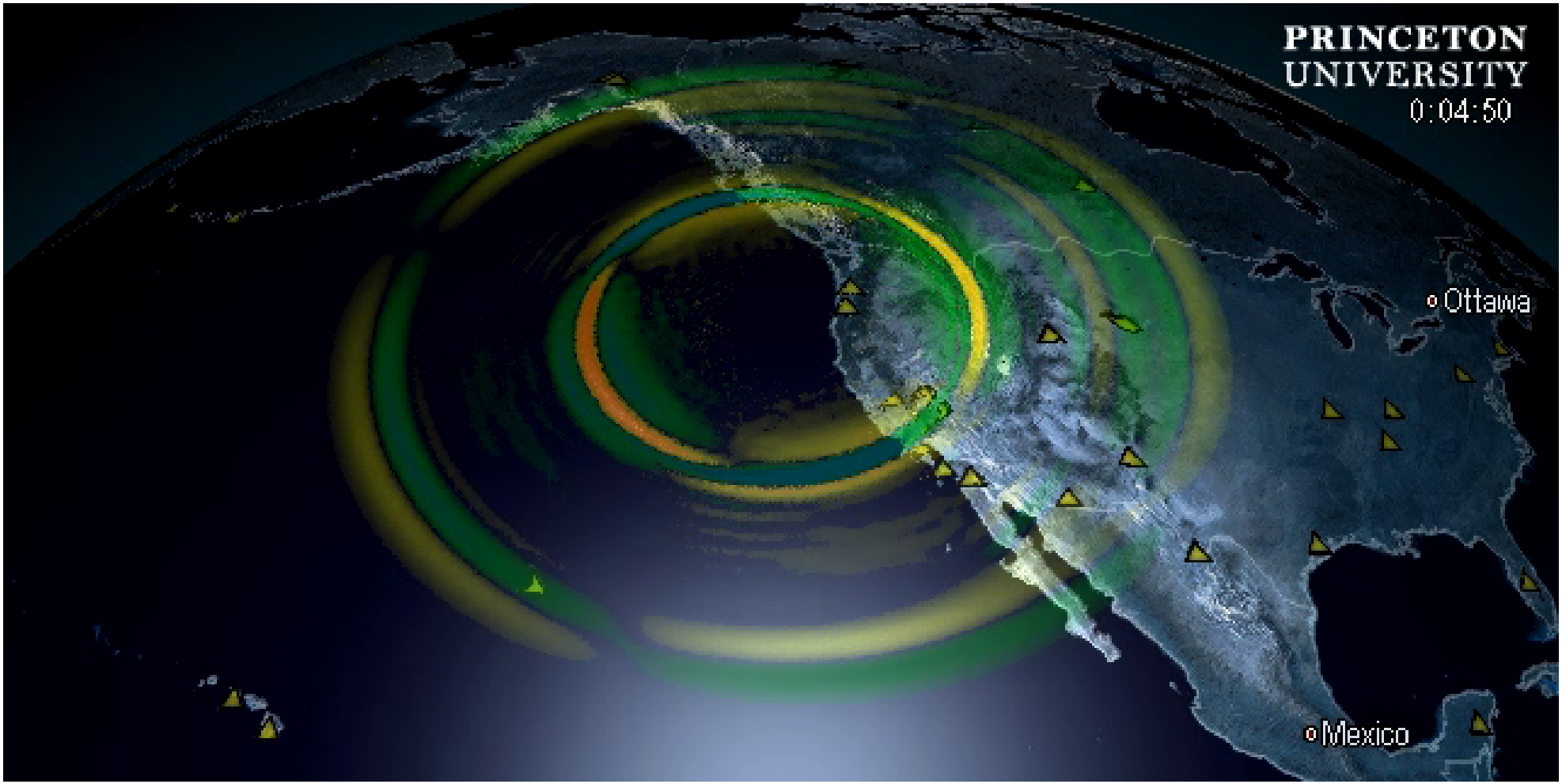

Forward modeling using SPECFEM3D_GLOBE

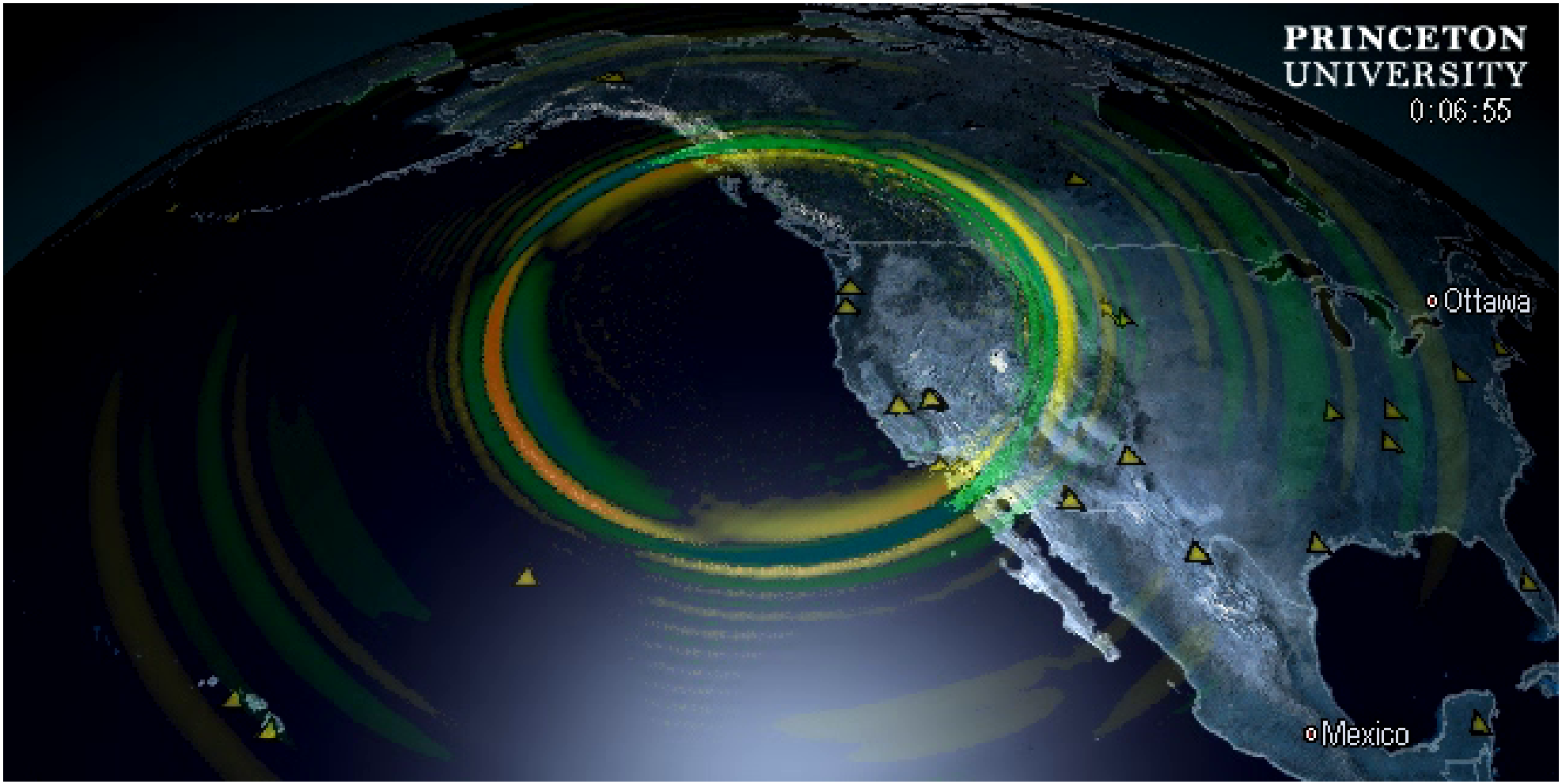

Forward modeling using SPECFEM3D_GLOBE

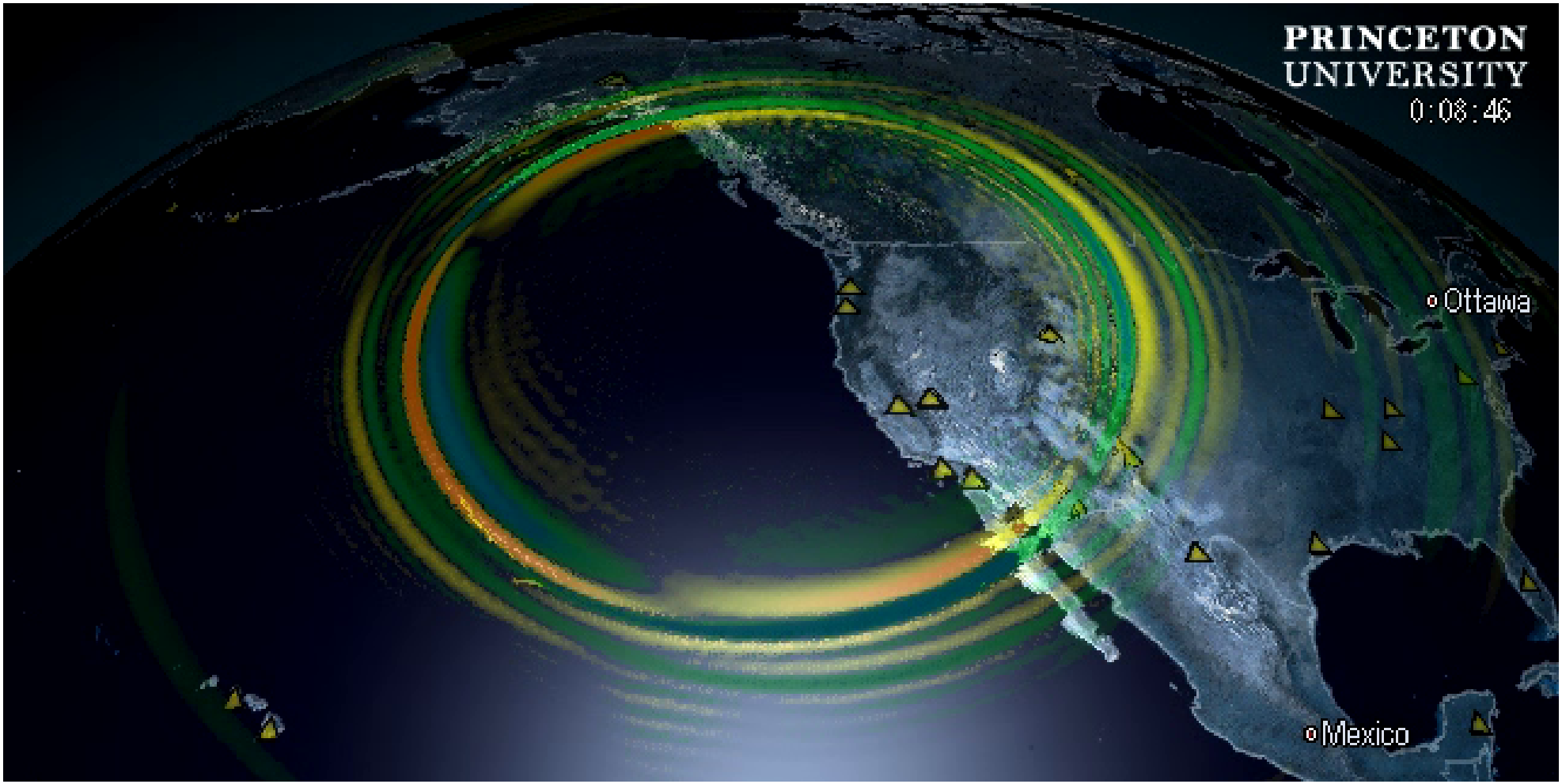

Forward modeling using SPECFEM3D_GLOBE

Forward modeling using SPECFEM3D_GLOBE

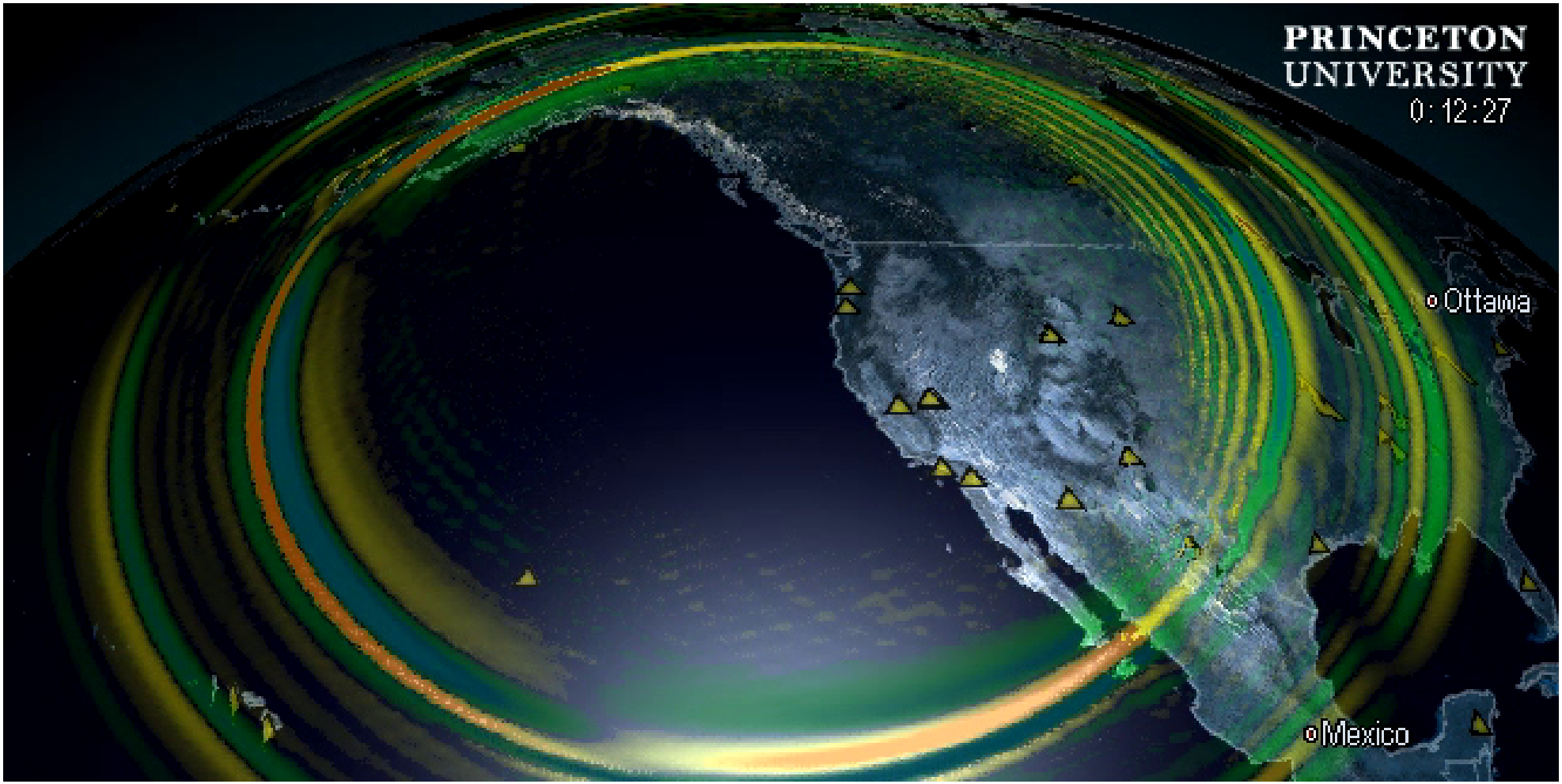

Forward modeling using SPECFEM3D_GLOBE

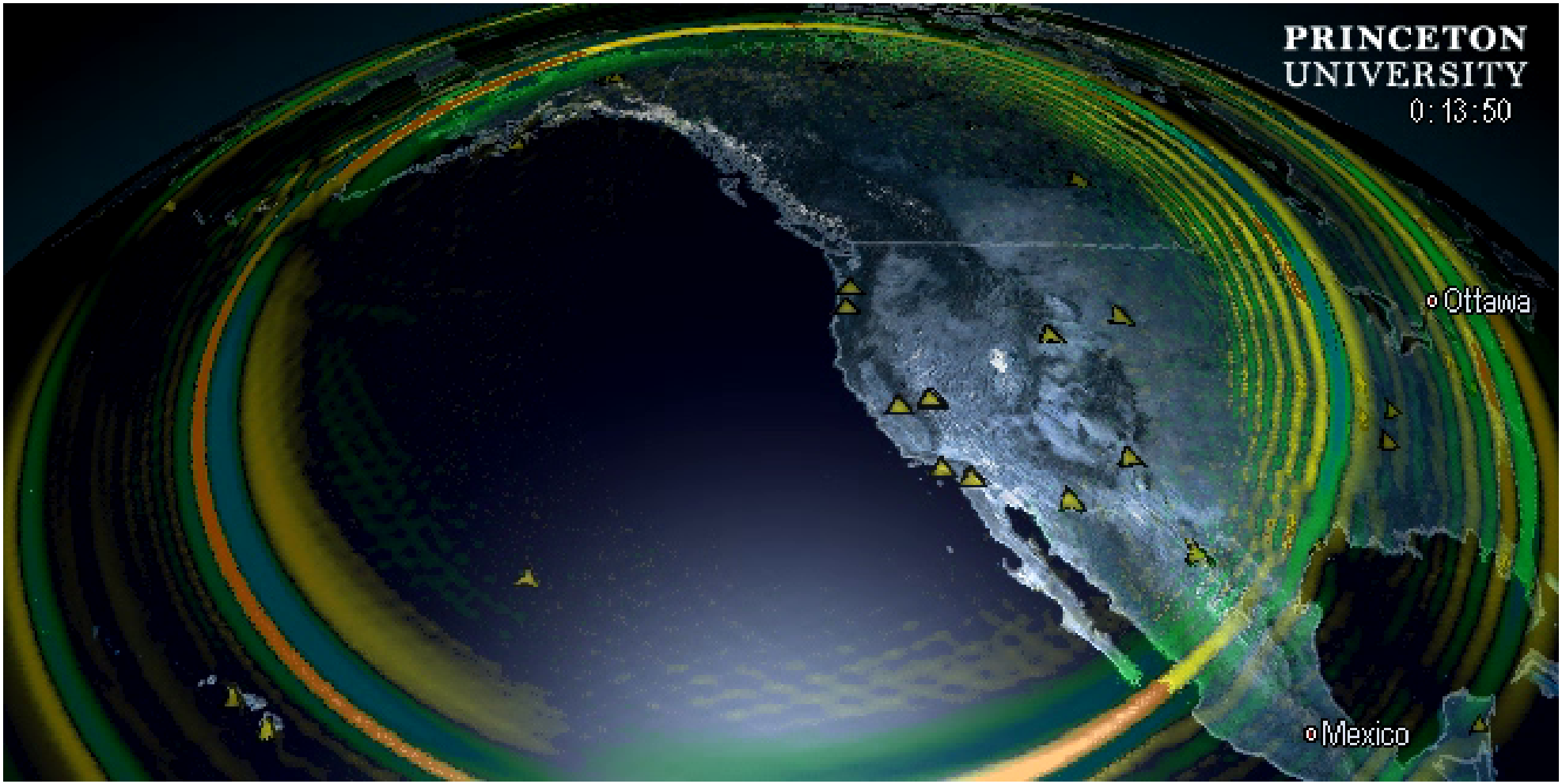

Forward modeling using SPECFEM3D_GLOBE

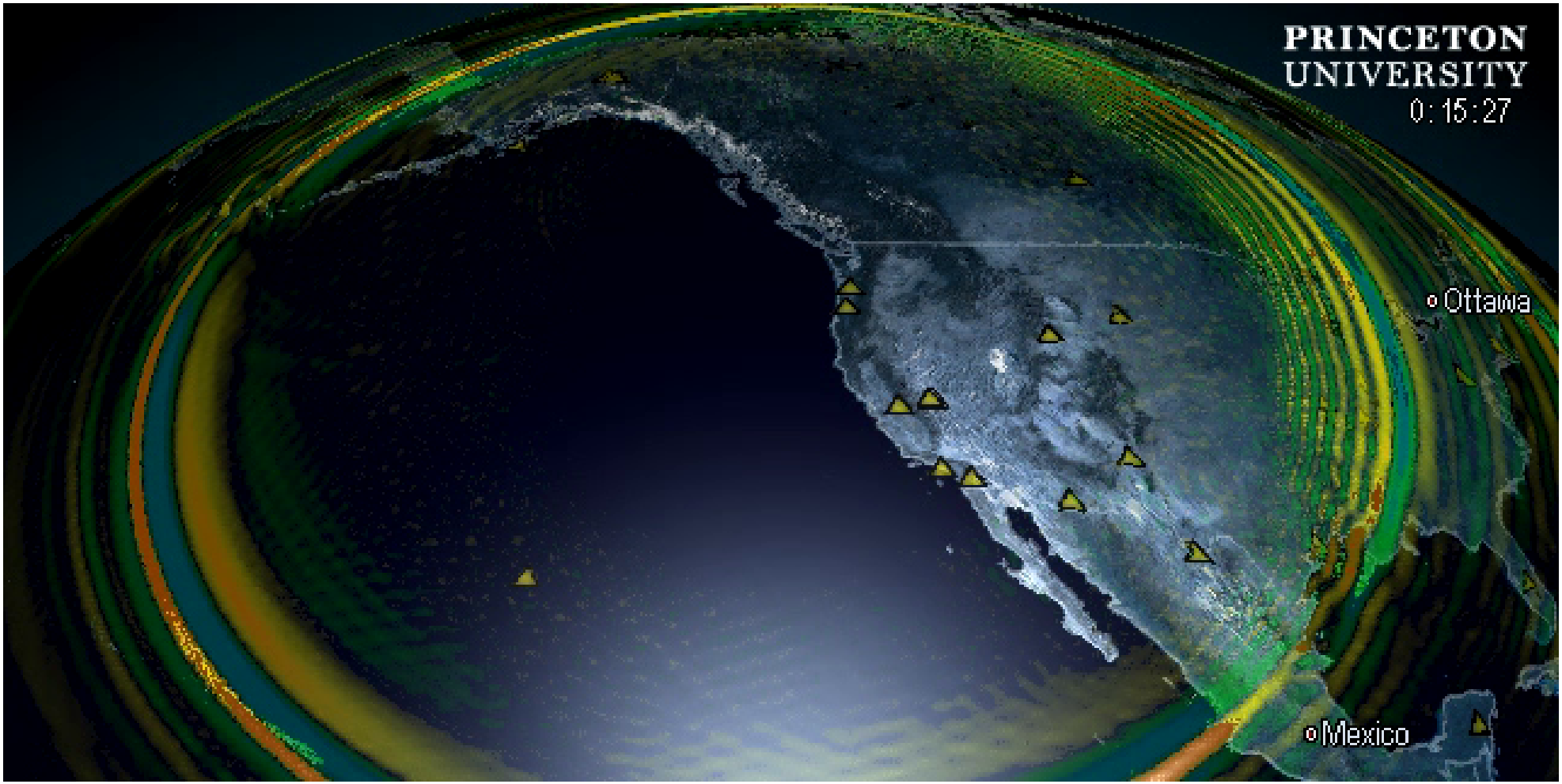

Forward modeling using SPECFEM3D_GLOBE

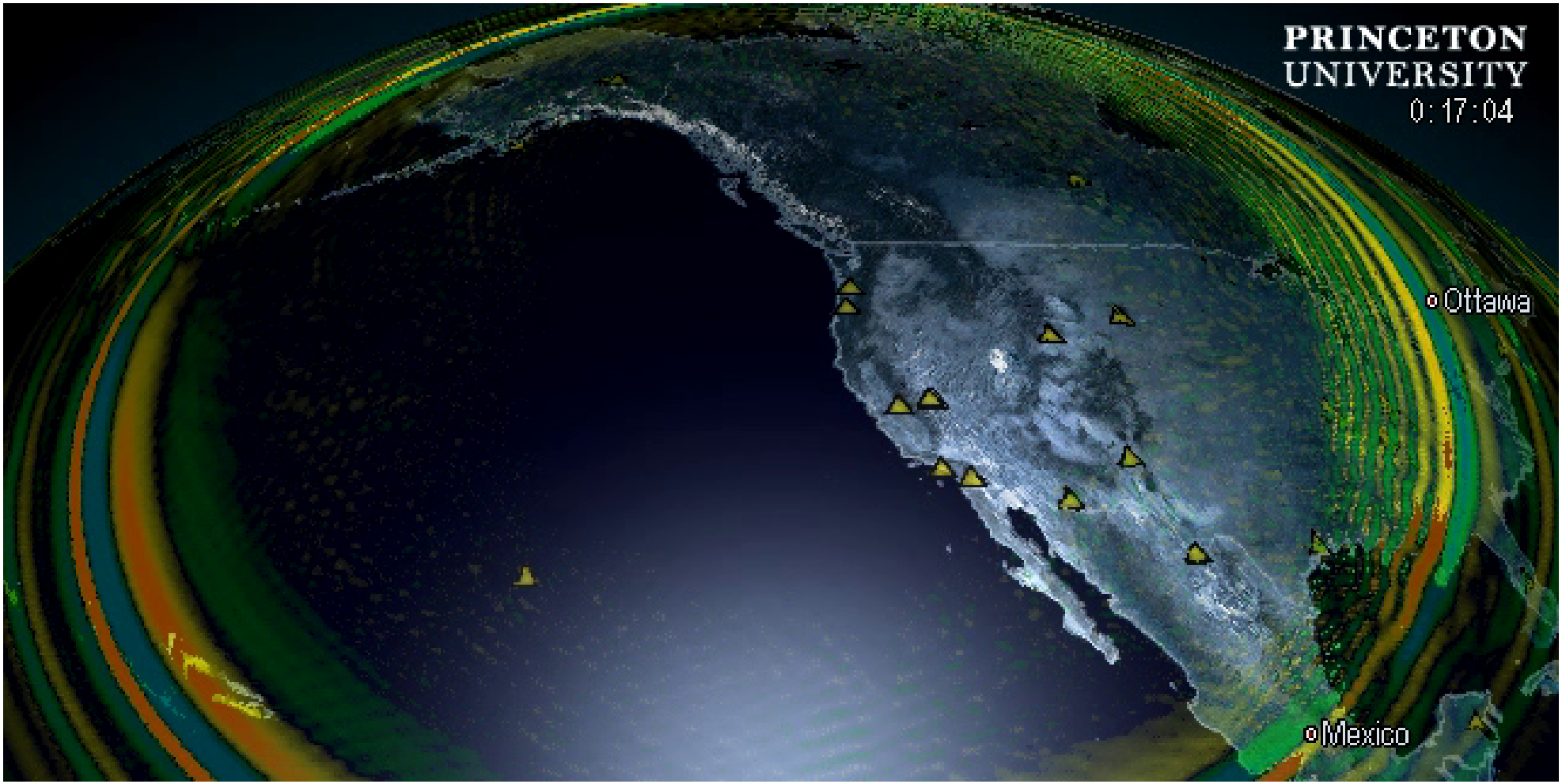

Forward modeling using SPECFEM3D_GLOBE

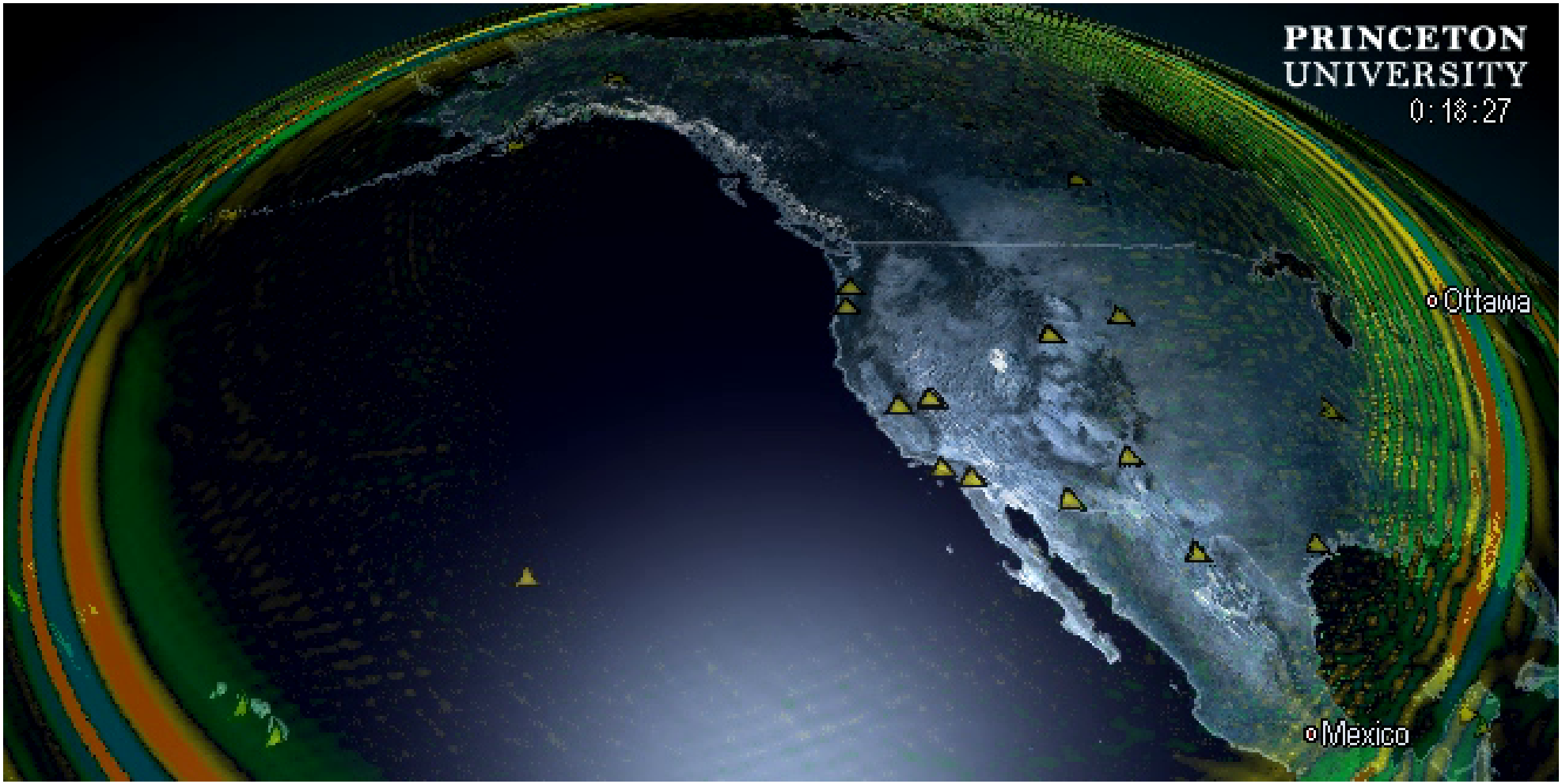

Forward modeling using SPECFEM3D_GLOBE

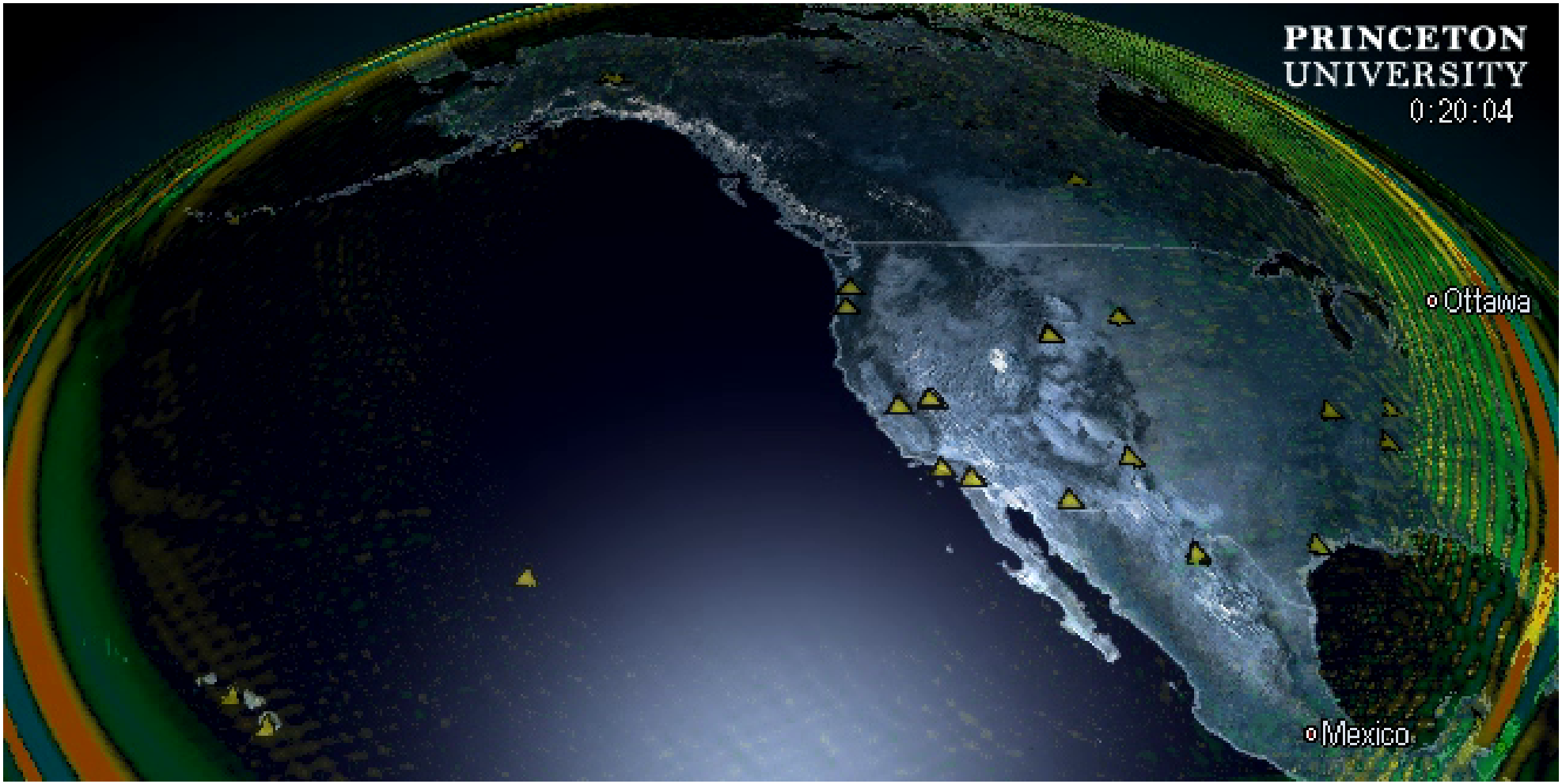

Forward modeling using SPECFEM3D_GLOBE

Forward modeling using SPECFEM3D_GLOBE

Forward modeling using SPECFEM3D_GLOBE

Any seismogram

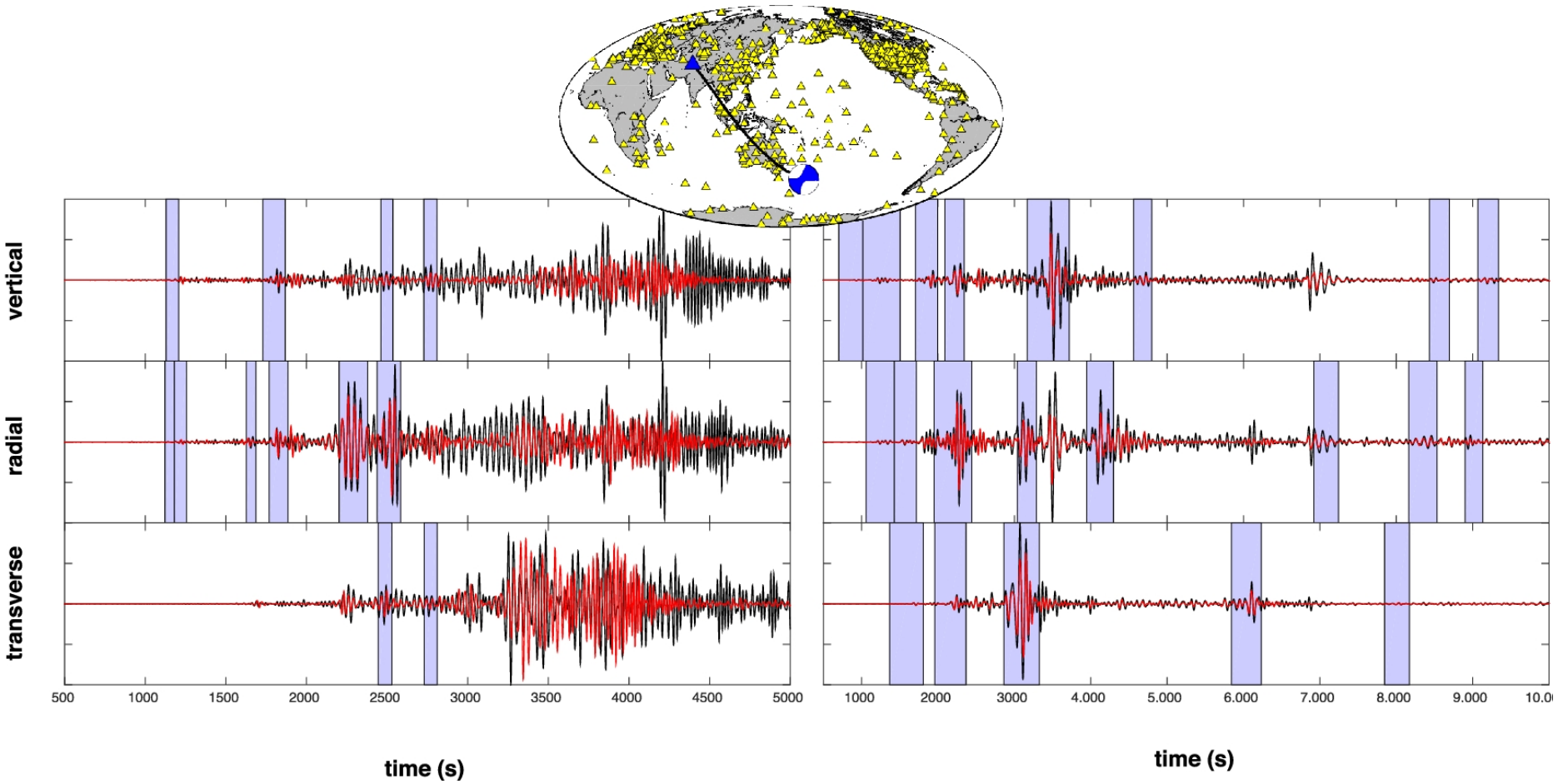

Bozdağ et al. (2016)

Any phase

Modern (e.g. SEM) methods can compute wavefields in *arbitrary* 3D background models. We no longer have to assume that only P (or S) wave speed perturbations influence P (or S) cross-correlation travel times of P (or S) waveforms.

Any phase

Modern (e.g. SEM) methods can compute wavefields in *arbitrary* 3D background models. We no longer have to assume that only P (or S) wave speed perturbations influence P (or S) cross-correlation travel times of P (or S) waveforms.

We can take one step back and restart from the **Born approximation** (8–9):

$$\delta u(t) = \iiint_{\text{Earth}} \left\{ K_{\rho}^{\delta u}(t) \left(\frac{\delta \rho}{\rho_0} \right) + K_{\mathbf{C}}^{\delta u}(t) \left(\frac{\delta \mathbf{C}}{\mathbf{C}_0} \right) \right\} dV, \tag{11}$$

where computing **3D waveform kernels** involves **one forward simulation** and **one backward simulation** and their interaction by **convolution**:

Any phase

Modern (e.g. SEM) methods can compute wavefields in *arbitrary* 3D background models. We no longer have to assume that only P (or S) wave speed perturbations influence P (or S) cross-correlation travel times of P (or S) waveforms.

We can take one step back and restart from the **Born approximation** (8–9):

$$\delta u(t) = \iiint_{\text{Earth}} \left\{ K_{\rho}^{\delta u}(t) \left(\frac{\delta \rho}{\rho_0} \right) + K_{\mathbf{C}}^{\delta u}(t) \left(\frac{\delta \mathbf{C}}{\mathbf{C}_0} \right) \right\} dV, \tag{11}$$

where computing **3D waveform kernels** involves **one forward simulation** and **one backward simulation** and their interaction by **convolution**:

$$K_{\rho}^{\delta u}(t) = -\int_0^t \dot{u}_i^{\text{to}}(\tau)\, \dot{u}_i^{\text{fro}}(t-\tau)\, d\tau, \tag{12}$$

$$K_{\mathbf{C}}^{\delta u}(t) = -\int_0^t \epsilon_{ij}^{\text{to}}(\tau)\, \epsilon_{kl}^{\text{fro}}(t-\tau)\, d\tau. \tag{13}$$

Marquering et al. (1998); *Tromp et al.* (2005); *Nissen-Meyer et al.* (2007a,b); *Tape et al.* (2007)

Any kernel

Different flavors of SEM wavefield computation can be used...

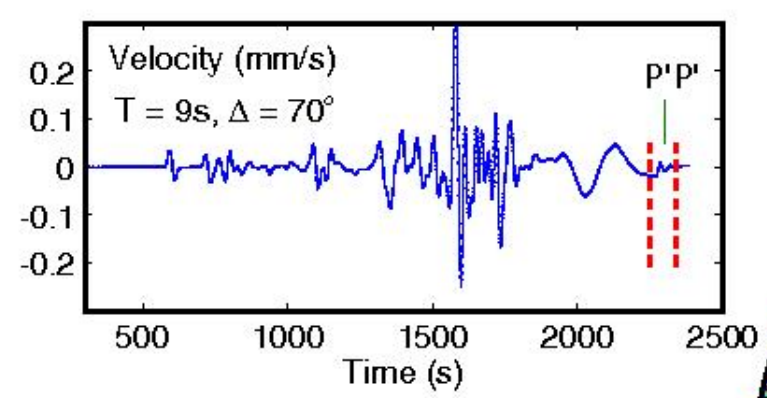

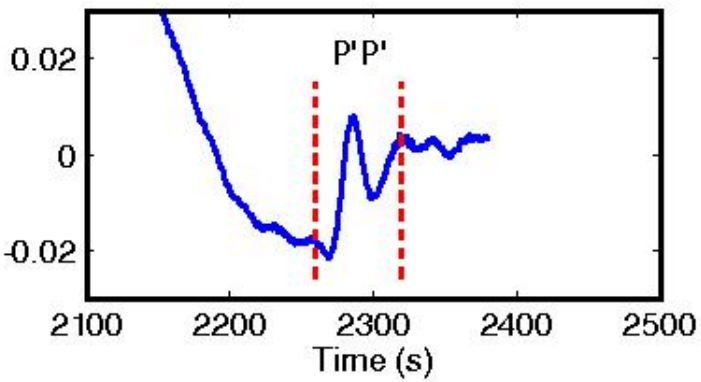

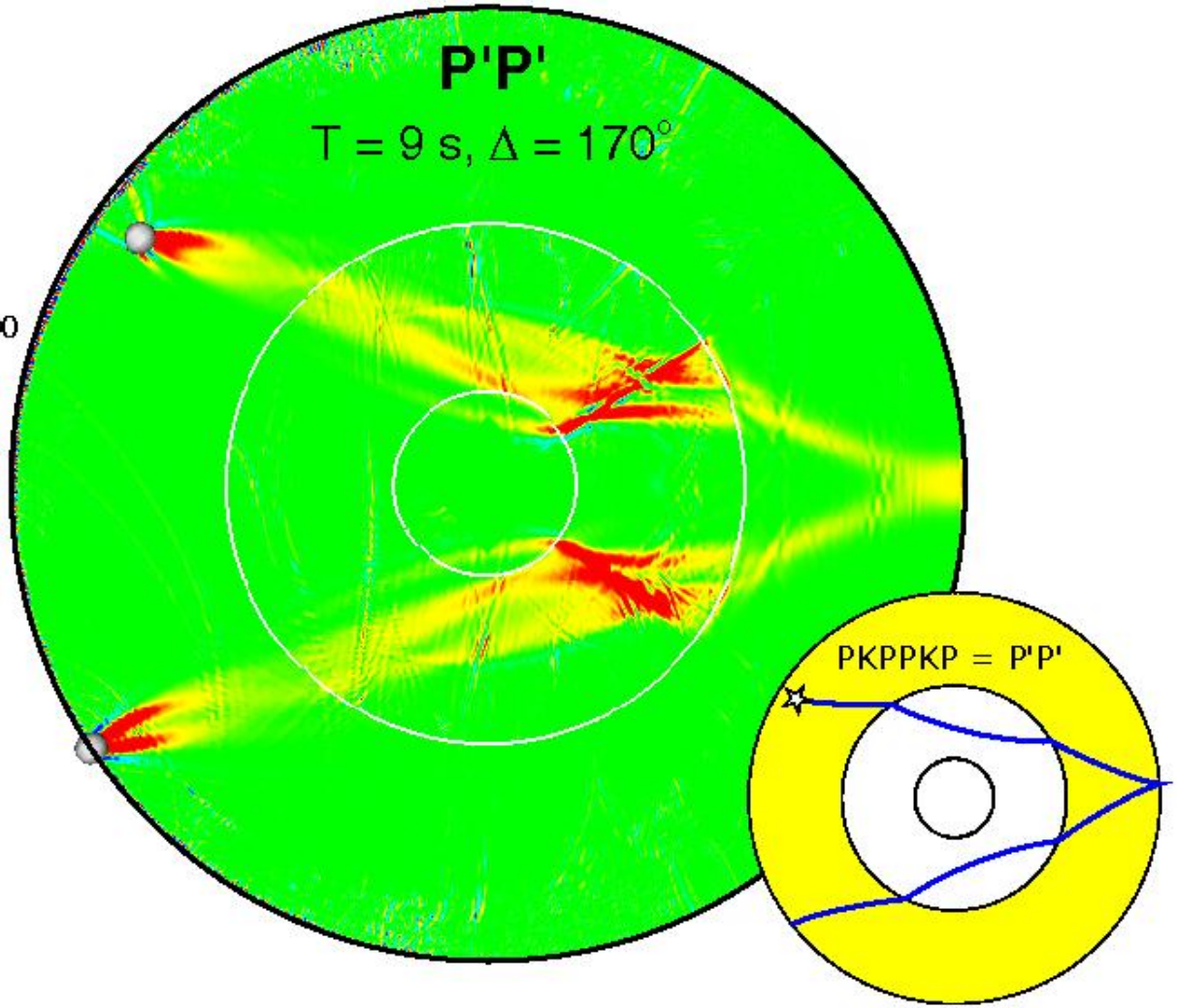

Tromp et al. (2005); *Nissen-Meyer et al.* (2007a,b); *Tape et al.* (2007)

Global models — III

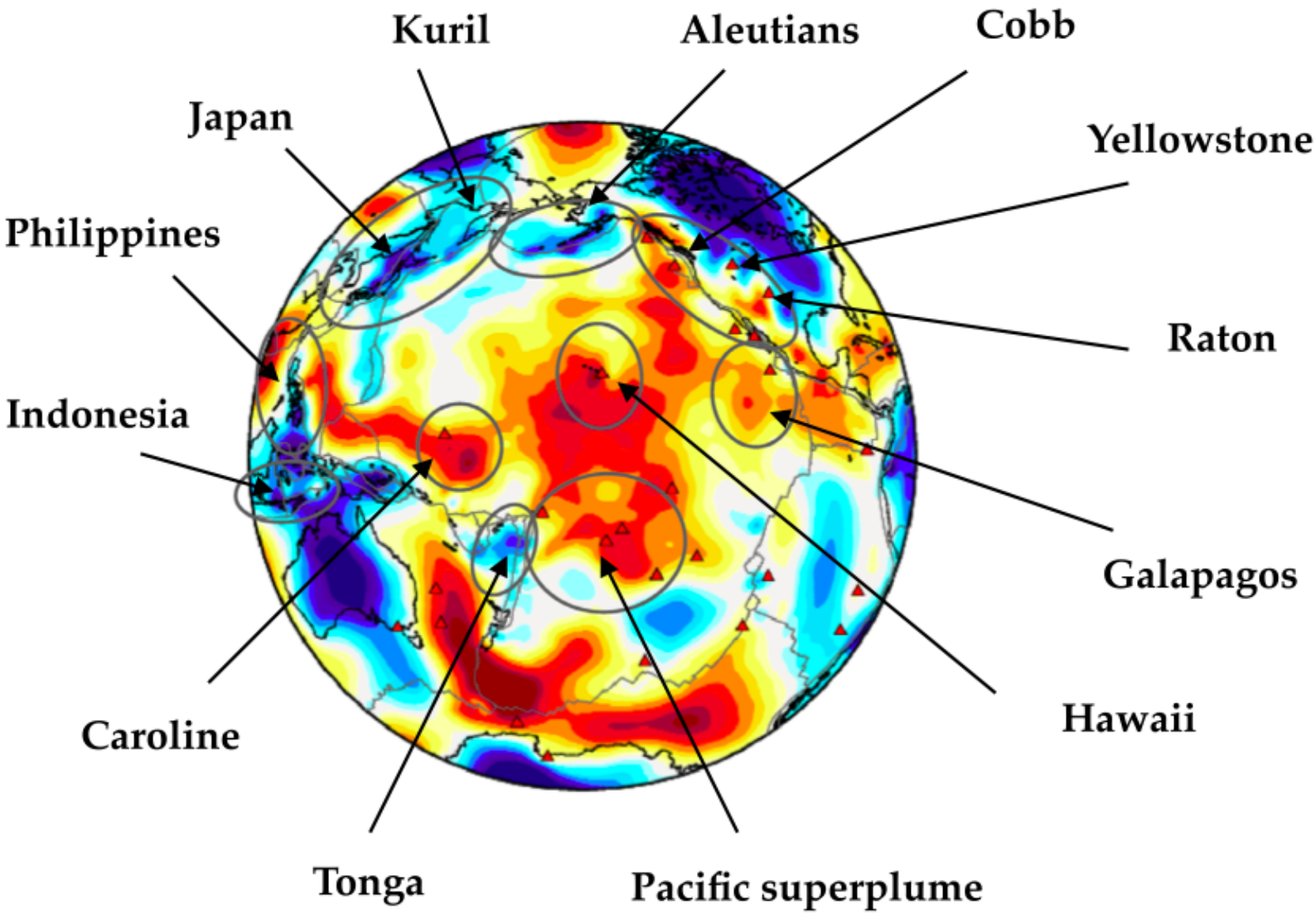

Bozdağ et al. (2016)

Any misfit metric

The *adjoint* method generalizes all of the above technology to the point where **any sort of aggregate misfit measure**, χ, can be optimized: (relative) *travel times*, *waveform*, *phase*, and *envelope* (double) differences...

Any misfit metric

The *adjoint* method generalizes all of the above technology to the point where **any sort of aggregate misfit measure**, χ, can be optimized: (relative) *travel times*, *waveform*, *phase*, and *envelope* (double) differences...

In the time-domain, the generic canonical **sensitivity kernel** for χ in the sense

$$\delta\chi = \int_V \left\{ K^{\chi}_{\rho}(\mathbf{x}) \frac{\delta\rho(\mathbf{x})}{\rho_0(\mathbf{x})} + K^{\chi}_{\mathbf{C}}(\mathbf{x}) \frac{\delta\mathbf{C}(\mathbf{x})}{\mathbf{C}_0(\mathbf{x})} \right\} dV, \tag{14}$$

is a wavefield **correlation-based** measure that involves a *forward propagating* wavefield u and *backward propagating* **adjoint** wavefield $u^{\dagger}$, for some T and $\Delta\tau$,

$$K^{\chi}(\mathbf{x}) \sim \int_0^{\Delta\tau} u(\mathbf{x}, T + \Delta\tau - \tau)\, u^{\dagger}(\mathbf{x}, \tau + T)\, d\tau. \tag{15}$$

The adjoint wavefield is excited by an **adjoint source** that measures data misfit.

Tromp et al. (2005, 2008); *Liu and Tromp* (2008); *Liu and Gu* (2012); *Yuan et al.* (2016, 2019); *Liu et al.* (2023)

Source encoding

In the frequency domain ($u \to \tilde{u}$, $t \to \omega$), over all sources, eq. (15) amounts to

$$K^{\chi}(\mathbf{x}) \sim \sum_{s=1}^{N_s} \sum_{k=1}^{N_\omega} \sum_{k'=1}^{N_\omega} \tilde{u}_s(\mathbf{x}, \omega_k)\, \tilde{u}_s^{\dagger *}(\mathbf{x}, \omega_k'). \tag{16}$$

This kernel controls the overall **misfit gradient**: the summation is over all seismic *sources* and all of their *frequencies*, and the basis of **iterative optimization**.

Source encoding

In the frequency domain ($u \rightarrow \tilde{u}$, $t \rightarrow \omega$), over all sources, eq. (15) amounts to

$$K^{\chi}(\mathbf{x}) \sim \sum_{s=1}^{N_s} \sum_{k=1}^{N_\omega} \sum_{k'=1}^{N_\omega} \tilde{u}_s(\mathbf{x}, \omega_k)\, \tilde{u}_s^{\dagger *}(\mathbf{x}, \omega_k'). \tag{16}$$

This kernel controls the overall **misfit gradient**: the summation is over all seismic *sources* and all of their *frequencies*, and the basis of **iterative optimization**.

Source encoding is a device whereby *individual* source frequencies are "tagged", e.g., $\tilde{u}_s(\mathbf{x}, \omega_k) \rightarrow \alpha_s(\omega_k)\tilde{u}_s(\mathbf{x}, \omega_k)$, such that the **order of summation** can be switched *without penalty*, for an **enormous gain** in computational efficiency:

$$\widetilde{K}^{\chi}(\mathbf{x}) = \sum_{k=1}^{N_\omega} \left[\sum_{s=1}^{N_s} \alpha_s(\omega_k)\tilde{u}_s(\mathbf{x}, \omega_k) \right] \left[\sum_{s'=1}^{N_s} \alpha_{s'}(\omega_k)\tilde{u}_{s'}^{\dagger}(\mathbf{x}, \omega_k) \right]^* . \tag{17}$$

Romero+2000

Laplace-domain Encoding & Time-domain Solvers

We encode single frequencies with *exponential prefactors* that can be **damped** (γ) and **shifted** (t_0^{sr}) for phase selectivity. We obtain expressions for the **forward field**

$$u_j(\mathbf{x}, t+T) = \sum_{s=1}^{S} \int_{-\infty}^{T+t} G_{ji}(\mathbf{x}, \mathbf{x_s}, T+t-t')\, f_i(\mathbf{x_s}, t)\, dt', \tag{18}$$

driven by a *monochromatic* source $f_i(\mathbf{x_s}, t) = \hat{n}_i(\mathbf{x_s})\, e^{\gamma t'} \sin \omega_s t'$. Note that G_{ji} is the Green's function.

Laplace-domain Encoding & Time-domain Solvers

We encode single frequencies with *exponential prefactors* that can be **damped** (γ) and **shifted** (t_0^{sr}) for phase selectivity. We obtain expressions for the **forward field**

$$u_j(\mathbf{x}, t+T) = \sum_{s=1}^{S} \int_{-\infty}^{T+t} G_{ji}(\mathbf{x}, \mathbf{x_s}, T+t-t')\, f_i(\mathbf{x_s}, t)\, dt', \tag{18}$$

driven by a *monochromatic* source $f_i(\mathbf{x_s}, t) = \hat{n}_i(\mathbf{x_s})\, e^{\gamma t'} \sin \omega_s t'$. Note that G_{ji} is the Green's function. Likewise, the expression for the **adjoint field** is

$$u_j^\dagger(\mathbf{x}, t) = \sum_{r=1}^{R} \int_0^t G_{ji}(\mathbf{x}, \mathbf{x_r}, t-t') f_i^\dagger(\mathbf{x_r}, t')\, dt', \tag{19}$$

driven by **adjoint sources** that contain the weighted **misfit measurement** $\bar{\Delta}\widetilde{u}_i^{sr}$,

$$f_i^\dagger(\mathbf{x_r}, t) = \sum_{s=1}^{S} e^{\gamma t_0^{sr}}\, \bar{\Delta}\widetilde{u}_i^{sr}\, e^{\imath\omega_s(T+t)} e^{-\gamma(T+t)}. \tag{20}$$

Global models — IV

The *art* is in the randomized frequency assignment scheme, the selection of the **integration interval** $\Delta\tau$, and determining the **steady-state time** T after which *mutual orthogonality* between suitably encoded frequencies is expected to set in.

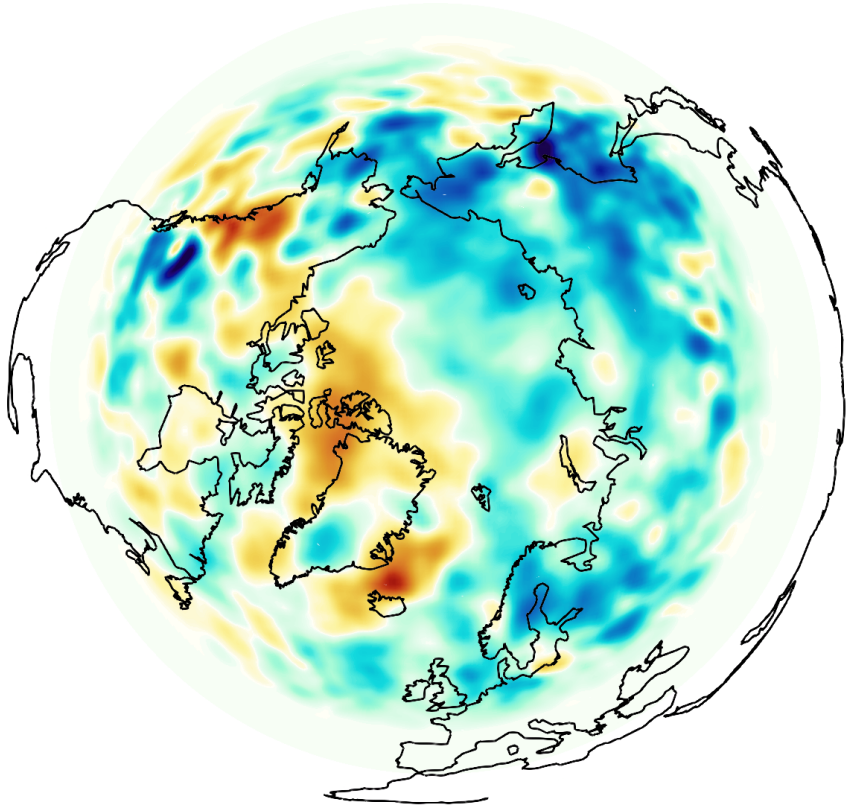

Tromp and Bachmann (2019); *Cui et al.* (2023); *Liu et al.* (2023)

Reflected phases

We discussed tomography based on **transmitted** phases. What about reflections?

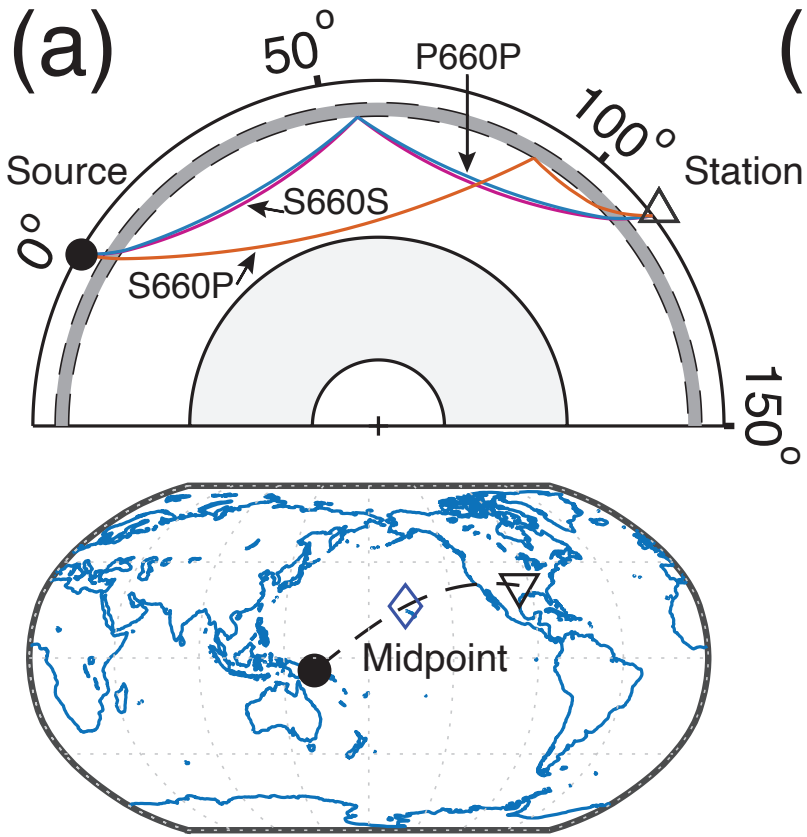

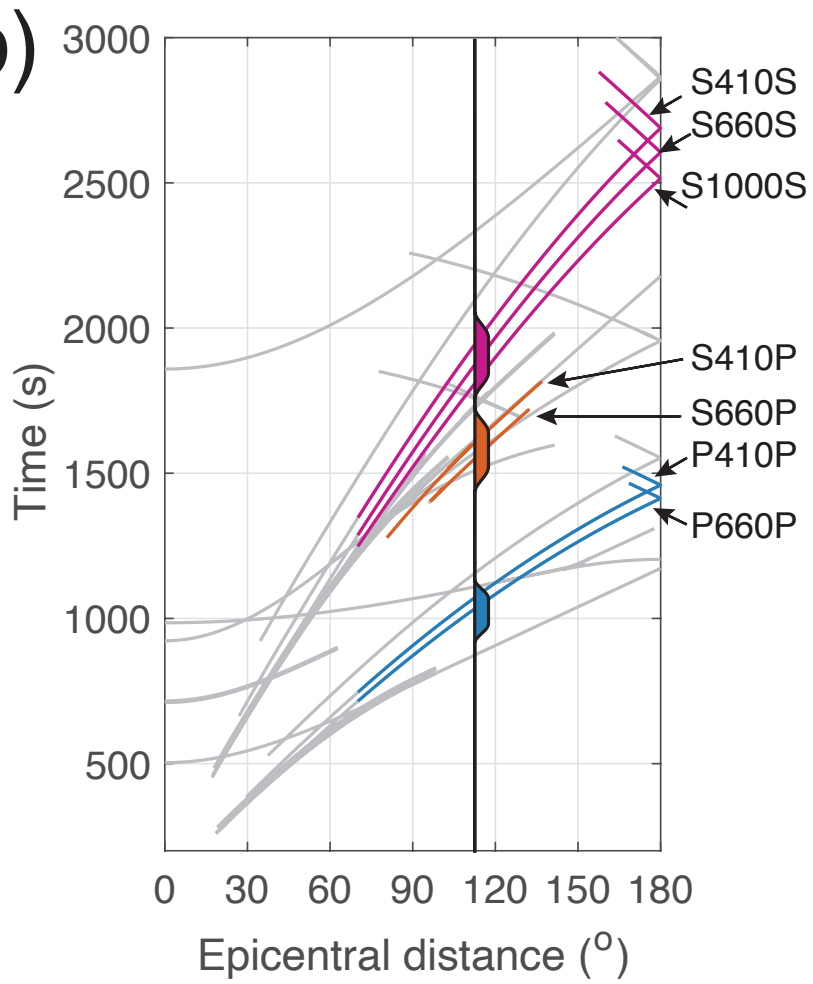

Zhang et al. (2023)

Impedance kernels

Underside **reflections** and **converted phases** image sharp discontinuities.

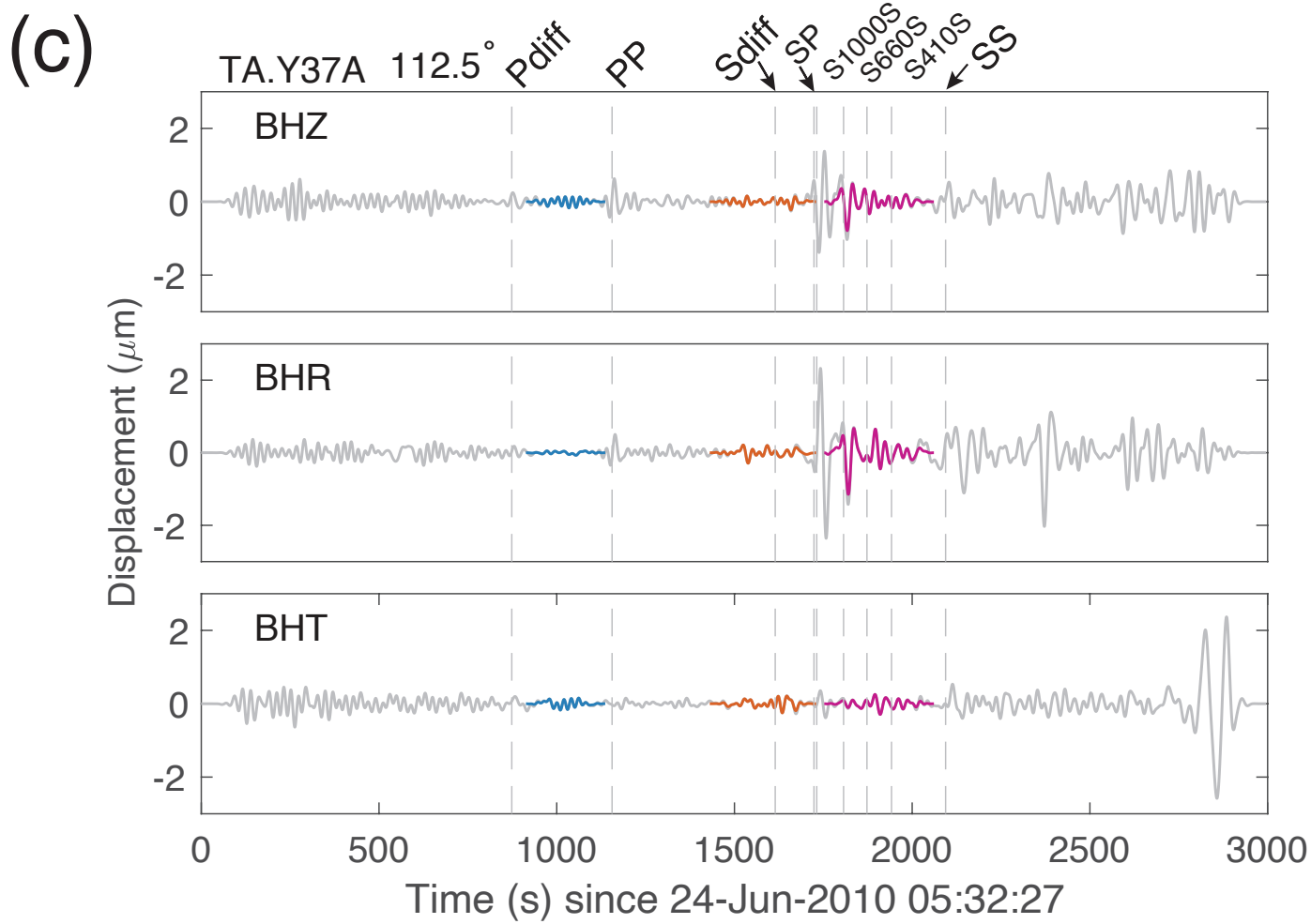

Zhang et al. (2023)

Impedance contrasts (including surprising ones)

Underside **reflections** and **converted phases** image sharp discontinuities.

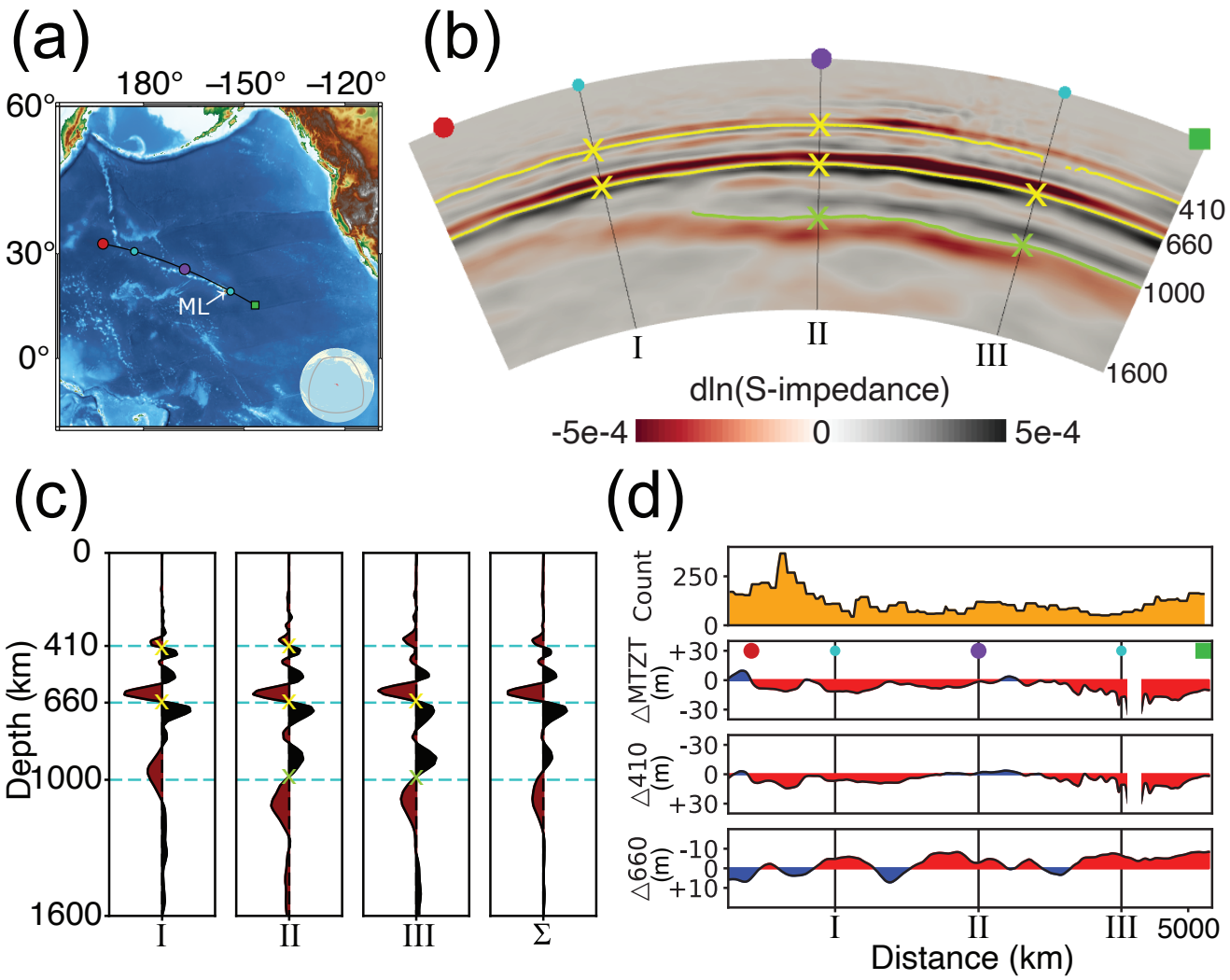

Zhang et al. (2023)

In conclusion:

Passive seismic imaging at all scales...

References

Aster, R. C., B. Borchers, and C. H. Thurber, *Parameter Estimation and Inverse Problems*, *International Geophysics Series*, vol. 90, Elsevier Academic Press, San Diego, Calif., 2005.

Astiz, L., P. S. Earle, and P. M. Shearer, Global stacking of broadband seismograms, *Seismol. Res. Lett.*, *67*(4), 8–18, 1996.

Bozdağ, E., D. Peter, M. Lefebvre, D. Komatitsch, J. Tromp, J. Hill, N. Podhorszki, and D. Pugmire, Global adjoint tomography: first-generation model, *Geophys. J. Int.*, *207*(3), 1739–1766, doi: 10.1093/gji/ggw356, 2016.

Bullen, K. E., and B. A. Bolt, *An Introduction to the Theory of Seismology*, 4 ed., Cambridge Univ. Press, Cambridge, UK, 1985.

Burky, A., J. C. E. Irving, and F. J. Simons, The mantle transition zone beneath eastern North America: Receiver functions and tomographic velocity models, *Phys. Earth Planet. Inter.*, *340*, 107,035, doi: 10.1016/j.pepi.2023.107,035, 2023.

Cui, C., E. Bachmann, D. B. Peter, Z. Liu, and J. Tromp, Source-encoded waveform inversion in the Northern Hemisphere, *Geophys. J. Int.*, *235*, 2305–2322, doi: 10.1093/gji/ggad363, 2023.

Dahlen, F. A., S.-H. Hung, and G. Nolet, Fréchet kernels for finite-frequency traveltimes — I. Theory, *Geophys. J. Int.*, *141*(1), 157–174, doi: 10.1046/j.1365–246X.2000.00,070.x, 2000.

Dziewoński, A. M., and D. L. Anderson, Preliminary Reference Earth Model, *Phys. Earth Planet. Inter.*, *25*, 297–356, doi: 10.1016/0031–9201(81)90,046–7, 1981.

Ekström, G., M. Nettles, and A. M. Dziewonski, The global CMT project 2004–2010: Centroid-moment tensors for 13,017 earthquakes, *Phys. Earth Planet. Inter.*, *200–201*, 1–9, doi: 10.1016/j.pepi.2012.04.002, 2012.

Fournier, A., H.-P. Bunge, R. Hollerbach, and J.-P. Vilotte, Application of the spectral-element method to the axisymmetric Navier-Stokes equation, *Geophys. J. Int.*, *156*, 682–700, doi: 10.1111/j.1365–246X.2004.02,149.x, 2004.

Hung, S.-H., F. A. Dahlen, and G. Nolet, Fréchet kernels for finite-frequency traveltimes — II. Examples, *Geophys. J. Int.*, *141*(1), 175–203, doi: 10.1046/j.1365–246X.2000.00,072.x, 2000.

Hung, S.-H., F. A. Dahlen, and G. Nolet, Wavefront healing: a banana-doughnut perspective, *Geophys. J. Int.*, *146*, 289–312, doi: 10.1046/j.1365–246x.2001.01,466.x, 2001.

Kennett, B. L. N., and E. R. Engdahl, Traveltimes for global earthquake location and phase identification, *Geophys. J. Int.*, *105*, 429–465, 1991.

Komatitsch, D., and J. Tromp, Introduction to the spectral element method for three-dimensional seismic wave propagation, *Geophys. J. Int.*, *139*(3), 806–822, doi: 10.1046/j.1365–246x.1999.00,967.x, 1999.

Komatitsch, D., and J. Tromp, Spectral-element simulations of global seismic wave propagation — I. Validation, *Geophys. J. Int.*, *149*(2), 390–412, doi: 10.1046/j.1365–246X.2002.01,653.x, 2002a.

Komatitsch, D., and J. Tromp, Spectral-element simulations of global seismic wave propagation — II. Three-dimensional models, oceans, rotation and self-gravitation, *Geophys. J. Int.*, *150*(1), 303–318, doi: 10.1046/j.1365–246X.2002.01,716.x, 2002b.

Komatitsch, D., and J. P. Vilotte, The spectral element method: An efficient tool to simulate the seismic response of 2D and 3D geological structures, *B. Seismol. Soc. Am.*, *88*(2), 368–392, doi: 10.1785/BSSA0880020,368, 1998.

Komatitsch, D., J. Ritsema, and J. Tromp, The spectral-element method, Beowulf computing, and global seismology, *Science*, *298*(5599), 1737–1742, doi: 10.1126/science.1076,024, 2002.

Liu, Q., and Y. J. Gu, Seismic imaging: From classical to adjoint tomography, *Tectonophysics*, *566–567*, 31–66, doi: 10.1016/j.tecto.2012.07.006, 2012.

Liu, Q., and J. Tromp, Finite-frequency sensitivity kernels for global seismic wave propagation based upon adjoint methods, *Geophys. J. Int.*, *174*, 265–286, doi: 10.1111/j.1365–246X.2008.03,798.x, 2008.

Liu, Z., J. Hoffmann, E. Bachmann, C. Cui, F. J. Simons, and J. Tromp, Laplace-domain crosstalk-free source-encoded elastic Full Waveform Inversion using time-domain solvers, *Geophysics*, p. under revision, 2023.

Luo, Y., and G. T. Schuster, Wave-equation traveltime inversion, *Geophysics*, *56*(5), 654–663, doi: 10.1190/1.1443,081, 1991.

Marquering, H., G. Nolet, and F. A. Dahlen, Three-dimensional waveform sensitivity kernels, *Geophys. J. Int.*, *132*(3), 521–534, doi: 10.1046/j.1365–246X.1998.00,426.x, 1998.

Marquering, H., F. A. Dahlen, and G. Nolet, Three-dimensional sensitivity kernels for finite-frequency travel times: the banana-doughnut paradox, *Geophys. J. Int.*, *137*(3), 805–815, doi: 10.1046/j.1365–246x.1999.00,837.x, 1999.

Menke, W., *Geophysical Data Analysis: Discrete Inverse Theory*, *International Geophysics Series*, vol. 45, Rev. ed., Academic Press, San Diego, Calif., 1989.

Montelli, R., G. Nolet, F. A. Dahlen, G. Masters, E. R. Engdahl, and S.-H. Hung, Finite-frequency tomography reveals a variety of plumes in the mantle, *Science*, *303*(5656), 338–343, doi: 10.1126/science.1092,485, 2004.

Nissen-Meyer, T., F. A. Dahlen, and A. Fournier, Spherical-earth Fréchet sensitivity kernels, *Geophys. J. Int.*, *168*(3), 1051–1066, doi: 10.1111/j.1365–246X.2006.03,123.x, 2007a.

Nissen-Meyer, T., A. Fournier, and F. A. Dahlen, A two-dimensional spectral-element method for computing spherical-earth seismograms — I. Moment-tensor source, *Geophys. J. Int.*, *168*(3), 1067–1092, doi: 10.1111/j.1365–246X.2006.03,121.x, 2007b.

Nissen-Meyer, T., M. van Driel, S. C. Stähler, K. Hosseini, S. Hempel, L. Auer, A. Colombi, and A. Fournier, AxiSEM: broadband 3-D seismic wavefields in axisymmetric media, *Solid Earth*, *5*(1), 425–445, doi: 10.5194/se–5–425–2014, 2014.

Nolet, G. (Ed.), *Seismic Tomography*, Reidel, Hingham, Mass., 1987.

Radon, J., Über die Bestimmung von Funktionen durch ihre Intergralwerte längs gewisser Mannigfaltigkeiten, *Berichte Sächsische Akademie der Wissenschaften*, *29*, 262–277, 1917.

Shearer, P. M., *Introduction to Seismology*, 3 ed., Cambridge Univ. Press, Cambridge, UK, 2019.

Simmons, N. A., S. C. Myers, G. Johannesson, and E. Matzel, LLNL-G3Dv3: Global P wave tomography model for improved regional and teleseismic travel time prediction, *J. Geophys. Res.*, *117*, B10,302, doi: 10.1029/2012JB009,525, 2012.

Tape, C., Q. Liu, and J. Tromp, Finite-frequency tomography using adjoint methods — Methodology and examples using membrane surface waves, *Geophys. J. Int.*, *168*, 1105–1129, doi: 10.1111/j.1365–246X.2006.03,191.x, 2007.

Tromp, J., and E. Bachmann, Source encoding for adjoint tomography, *Geophys. J. Int.*, *218*(3), 2019–2044, doi: 10.1093/gji/ggz271, 2019.

Tromp, J., C. Tape, and Q. Liu, Seismic tomography, adjoint methods, time reversal and banana-doughnut kernels, *Geophys. J. Int.*, *160*(1), 195–216, doi: 10.1111/j.1365–246X.2004.02,453.x, 2005.

Tromp, J., D. Komatitsch, and Q. Liu, Spectral-element and adjoint methods in seismology, *Comm. Comput. Phys.*, *3*(1), 1–32, 2008.

Yoshizawa, K., and B. L. N. Kennett, Determination of the influence zone for surface wave paths, *Geophys. J. Int.*, *149*, 440–453, doi: 10.1046/j.1365–246X.2002.01,659.x, 2002.

Yuan, Y. O., F. J. Simons, and J. Tromp, Double-difference adjoint seismic tomography, *Geophys. J. Int.*, *206*(3), 1599–1618, doi: 10.1093/gji/ggw233, 2016.

Yuan, Y. O., E. Bozdağ, C. Ciardelli, F. Gao, and F. J. Simons, The exponentiated phase measurement, and objective-function hybridization for adjoint waveform tomography, *Geophys. J. Int.*, *221*(2), 1145–1164, doi: 10.1093/gji/ggaa063, 2019.

Zhang, Z., J. C. E. Irving, F. J. Simons, and T. Alkhalifah, Seismic evidence for a 100 km mantle discontinuity under the Pacific, *Nat. Commun.*, *14*, 1714, doi: 10.1038/s41,467–023–37,067–x, 2023.

Zhao, D., Importance of later phases in seismic tomography, *Phys. Earth Planet. Inter.*, *296*, 106,314, 10.1016/j.pepi.2019.106,314, 2019.

Zhao, D., and J. Lei, Seismic ray path variations in a 3D global velocity model, *Phys. Earth Planet. Inter.*, *141*, 153–166, 2004.

Zhao, L., and T. H. Jordan, Sensitivity of frequency-dependent traveltimes to laterally heterogeneous, anisotropic Earth structure, *Geophys. J. Int.*, *133*, 683–704, 1998.

Zhao, L., T. H. Jordan, and C. H. Chapman, Three-dimensional Fréchet differential kernels for seismic delay times, *Geophys. J. Int.*, *141*(3), 558–576, doi: 10.1046/j.1365–246x.2000.00,085.x, 2000.